SSRG International Journal of Electrical and Electronics Engineering
ISSN: 2348-8379/ https://doi.org/10.14445/23488379/IJEEE-V11I12P132

Volume 11 Issue 12, 335-360, December 2024

Review Article

Advanced Droop Control Strategies for Microgrid

Seema P. Diwan[1], Rajin M. Linus[2]

[1]*Walchand College of Engineering, Maharashtra, India.*
[1,2]*Sanjay Ghodawat University, Maharashtra, India.*

[1]*Corresponding Author : seema.diwan@walchandsangli.ac.in*

Received: 18 October 2024 Revised: 19 November 2024 Accepted: 16 December 2024 Published: 31 December 2024

Abstract *- This article reviews the current landscape of droop control methods in Microgrids (MG), specifically focusing on advanced, communication-less strategies that enhance real and reactive power sharing accuracy. While widely utilised, Conventional Droop Control (CDC) techniques often struggle with power sharing inaccuracies and dynamic response inefficiencies, particularly in systems with resistive, complex or mismatched line impedances. This review introduces a novel and systematic classification of advanced droop control strategies aimed at addressing these limitations. The proposed classification categorizes methods based on their ability to improve power-sharing precision in different scenarios, including Low-Voltage (LV) MGs with resistive lines, Medium-Voltage (MV) systems with complex feeder impedances, dynamic loading conditions, and mismatched line impedance scenarios. For example, virtual impedance-based droop methods enhance reactive power sharing in mismatched impedances, while reverse droop control improves power sharing in resistive LV networks. Power decoupling transforms are also employed to enhance power-sharing precision in complex and resistive MG. This review also provides an in-depth analysis of the CDC, with its limitations verified through extensive simulations. A comparative study of advanced droop methods based on key parameters clearly explains their applicability in various operational scenarios. The findings are validated through simulations, providing practical insights into using advanced droop control methods in MG.*

Keywords *- Microgrid, Conventional Droop Control, Active power sharing, Power management in microgrid, Reactive Power Sharing, Inaccuracies in power sharing, Classification of Droop Control.*

1. Introduction

Energy demand is increasing globally due to several interconnected factors such as urbanization, population growth demanding energy for transportation, heating, and cooling, industrialization in developed countries, and technological advances in many sectors leading to higher energy consumption [1]. The need to generate more electricity and the growing interest in greener technology drive the emergence of power distribution networks centered on renewable energy-based Distributed Generation (DG) units. [2–4]. DG units contribute to power grid stability, sustainability, and efficiency by reducing emissions, minimizing transmission losses, and promoting the adoption of local Renewable Energy Sources (RES). This enhances the resilience and capacity of the large-scale electrical infrastructure [5, 6]. DG units, however, can complicate the distribution network by causing reverse power flow, voltage level variations, and voltage instability. The aggregation of multiple DG units into an MG can effectively address these challenges [7], facilitating the widespread adoption of DG systems by enhancing their integration and operational stability within the power distribution framework [8]. Figure 1 shows the model of hybrid MG. It comprises RES-based DGs, such as photovoltaic arrays, wind turbines, Battery Energy Storage Systems (BESS), and different loads. DC to AC converters connect the solar PV arrays and BESS to the AC bus. Wind power plants can be tied to an AC bus utilizing back-to-back converters that convert DC to AC and AC to DC. MG can operate in islanding mode or grid-tied [9–11]. During islanding mode, MG is disconnected from the utility grid and the electrical energy needed for local loads is primarily provided by internal DG sources and their power converters. In grid tied mode, surplus power generated by DG units flows from the MG to the utility grid and can offer ancillary services.

If the power from the DG units is insufficient to meet the load demands of the utility grid, the power system supplements it by drawing power from the utility grid [12]. Efficient MG management, whether in grid-tied or islanding mode, requires advanced control strategies to ensure effective power management and sharing among DG units. By leveraging advanced control techniques, MGs can optimize the integration and utilization of RES, reducing dependency on fossil fuels and enhancing sustainability. Additionally, these methods ensure seamless coordination between DG units, contributing to the overall power system's economy, stability, and reliability, even during dynamic operating conditions or disturbances.

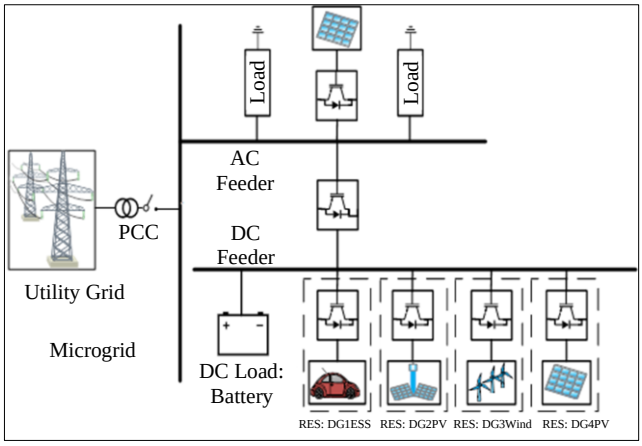

Fig. 1 Hybrid AC-DC MG

A fundamental challenge in MG management is achieving precise and efficient power sharing among DG units. Interfacing inverters, essential to power sharing control algorithms, interface different DGs, including photovoltaic panels, wind energy, and BESS, with the MG infrastructure [13]. Power sharing control approaches that operate independently of communication typically use the droop concept as their basis [14–17]. The operating principle of droop-based methods originates from traditional synchronous generators, balancing input and output power under steady-state conditions. In synchronous generators, when the mechanical input power exceeds the electrical output power ($Pm>Pe$), the generator's rotor accelerates, leading to an increase in frequency. Conversely, when ($Pm<Pe$), the rotor decelerates, causing the frequency to drop. Reactive power fluctuations similarly affect voltage magnitude, with increased demand causing voltage drops and reduced demand causing voltage rises. These steady-state variations in frequency and voltage serve as control parameters to regulate power flow. The droop method utilizes this principle, proportionally adjusting frequency and voltage in response to active and reactive power changes. Droop based power sharing mechanism can be artificially crafted for parallel connected converter-based DG units. It mimics the behavior of traditional synchronous generators by adjusting active power based on frequency (P-f) and reactive power based on voltage (Q-V). This enables proportional power sharing among DG units without relying on communication networks, making it ideal for MG applications.

1.1. Lierature Review

The use of droop characteristics to control DG units is widely documented in research studies [10, 18–21]. The CDC method implemented for DG units offers benefits like simple implementation and decentralized functioning. However, it faces several challenges in precise power sharing among parallel connected DG units. These challenges include ineffective distribution of harmonic power [22, 23] sub optimal performance in LV distribution networks due to a low reactance-to-resistance (X/R) ratio 7, 24], and the degraded real and reactive power sharing in complex and mismatched line impedance conditions [7, 24, 25]. Several advancements in CDC methods have been suggested to overcome these limitations. In resistive networks, CDC may reduce the accuracy of active power sharing. Decoupling methods like linear transformations [18, 24, 26] are used before applying CDC to fix this issue. A transformation frame based on the R/X ratio of the lines is used to calculate virtual powers. P/Q decoupling is possible if the system is purely inductive or the R/X ratio is known [26]. A virtual frequency and voltage frame is also proposed in [27–30], similar to [26]. An enhanced droop control technique is designed by adding a virtual negative impedance with the CDC approach [31]. In reference [7], a virtual inductor is proposed to estimate the voltage drops due to mismatched line impedance. This method improves the power sharing accuracy, specifically for LVMG with low X/R ratios.

In [32], a controller is proposed to address problems associated with complex impedance in MVMG. It simplifies the coupling between active and reactive power, improves dynamic performance, and works effectively when resistance and inductance are similar ($X \approx R$). In [29, 33], P-Q-V controis proposes improving voltage regulation and controlling power components at PCC. In reference [34], a supplementary loop is introduced to enhance the power-sharing capabilities by utilising high droop gains. This loop is designed to filter out the DC component, thus isolating the oscillatory behavior around the steady-state value of the real power output of each converter. In [35], droop coefficients are adjusted dynamically according to the loading condition instead of having constant values to improve power sharing precision and stability. A novel method to damp low frequency oscillations and improve power sharing using virtual inertia and adaptive frequency restoration loop is proposed in [15, 36]. Virtual inertia and damping are simulated by incorporating a time delay into the control system through a low pass filter, effectively replicating the effects of physical inertia. An improved Q-V̇ droop control is proposed, which uses the first-order derivative of the reactive power of the inverter and maintains the required reactive power. This control remains stable under the acceptable limit of droop coefficients. However, a further increment of the voltage droop coefficient could lead to instability. CDC has a linear relationship between power and frequency. The arctangent-based method [37] introduces a nonlinear relationship by incorporating an arctan function into the active power droop equation. This nonlinear approach allows the slope of the droop to vary with active power, providing a flexible response to changes in power. One of the drawbacks of this method is that if the local inverter controllers are not synchronized, the minor inaccuracies in their timing crystals can cause the inverters' frequencies to drift apart. In [38], virtual flux drooping is proposed instead of drooping the inverter output voltage. This approach avoids complex inner multi-loop feedback control. It also reduces frequency and voltage deviations to some extent.

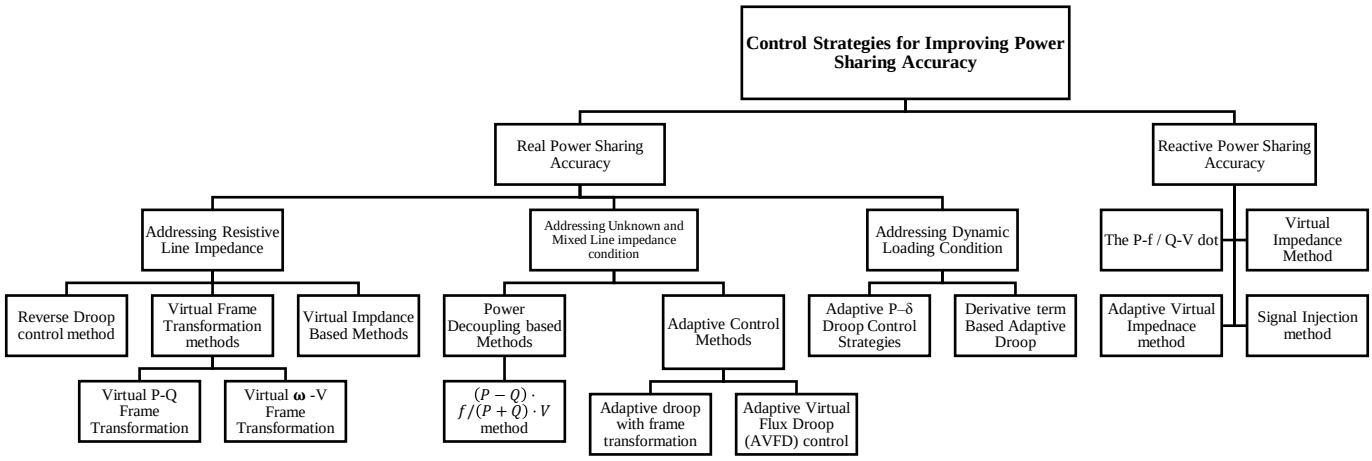

Fig. 2 Classification of advanced droop control methods

Many control methods have been suggested to adapt to the dynamic conditions in power systems and work with CDC to improve power sharing, dynamic and transient response and voltage regulation. In [39], a new adaptive voltage droop scheme is proposed for parallel DG operation in islanded AC MGs. This method adds two terms to the conventional Q-V control. One term compensates for the voltage drop across transmission lines. The other term adjusts the voltage droop for better performance. Control in [40] adaptively adjusts the reference voltage of each converter module. This is achieved by monitoring the reactive power drawn from each DG inverter module and adjusting the reference voltage to improve both voltage regulation and reactive power sharing performance. The concept of combining static and transient droop gains is proposed in [41]. The primary goal of the transient droop gains is to dampen low-frequency power-sharing modes. A mode-adaptive droop control approach is presented in [42], functioning effectively in both islanded and grid-connected conditions. In islanded mode, a derivative term for improved power loop dynamics is added to the P-f droop. During grid connection, integral control in the Q-V droop is used to achieve a better power factor.

In recent years, many review papers have been published summarizing the key characteristics of droop controllers and advancements in these techniques [43–47]. Review in [43] offers a broader examination of droop control techniques, discussing conventional methods alongside virtual impedance, adaptive, and robust droop controls. It includes a more general analysis of these strategies, touching on their benefits for managing DG units without focusing on specific improvements over CDC. In [44], a thorough review of control strategies across various MG types, examining the primary, secondary, and tertiary control layers and their unique demands. Ref. [45]comprehensively reviews control strategies for microgrid power converters, including concentrated control, master-slave control, droop mechanism, virtual synchronous generators, virtual oscillator control, distributed cooperative control, and model predictive control. References [46, 47] discuss control strategies for hybrid AC-DC MGs, highlighting their benefits and complexities. They outline hybrid MG power topologies and interlinking converters, systematically covering control strategies for objectives like modeling, power management, coordinated control, stability analysis, power quality, and protection. In summary, the surveyed literature extensively covers various aspects of power management strategies in MGs, focusing on theoretical frameworks and practical implementations. However, there remains a notable gap in the critical, detailed analysis of droop control variations and their systematic categorization for power sharing, which remains the focus of this review.

1.2. Problem Definition and Review Outline

While several modified droop control methods have been proposed to address the limitations of CDC, there is no comprehensive framework to categorize these methods systematically based on their specific challenges. This lack of a structured approach makes it difficult for researchers and practitioners to identify the most suitable control methodology for particular operational conditions in MG. To fill this gap, this review introduces a novel and systematic method for classifying the advanced droop control methodologies, as shown in Figure 2. It is designed to address specific issues that cause power-sharing inaccuracies in CDC under different operating conditions, such as low reactance-to-resistance (X/R) ratios, complex feeder impedances, dynamic load changes, and mismatched line impedances.

The classification highlights advanced droop methods targeting these issues, offering refined solutions to improve power sharing precision and operational stability. It also compares the performance of the methods on varying operation scenarios, highlighting their advantages and disadvantages. The categorization is constructed to offer clear, solution-oriented approaches to these problems.

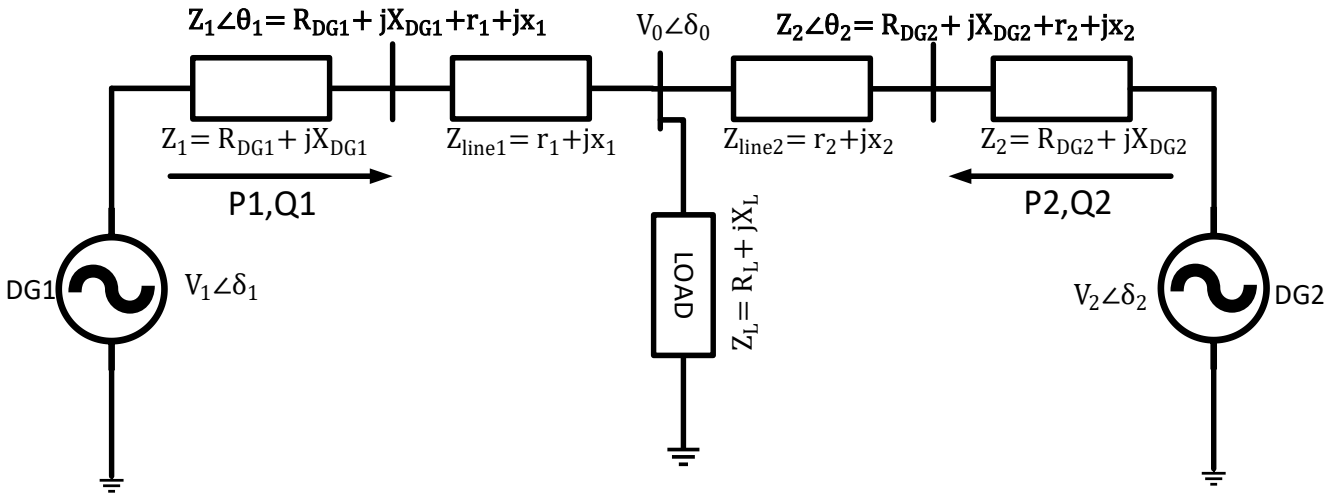

Fig. 3 Equivalent circuit of parallel connected inverters

For instance, each category within the framework is aligned with particular challenges associated with power sharing inaccuracies. This allows for a focused analysis of how each method contributes to enhancing the performance of MG. Through a detailed examination of each method's operational principle, strengths, and limitations, this paper seeks to provide a structured overview of the current state and future directions in droop control technologies for MG. This structured approach aims to guide future research and practical applications in developing and implementing efficient droop control strategies for MGs, bridging the gap between existing limitations and the growing demand for robust, decentralized power-sharing solutions. This review is organized in the following way: Section 2 outlines the basic principles of the CDC method and its inherent limitations in power sharing. The drawbacks are highlighted using extensive Simulink simulations. Section 3 provides a detailed categorization and analysis of the advantages and disadvantages of enhanced droop control adaptions designed to address each power sharing limitation of the CDC. Section 4 offers a comparative analysis and critical review of each CDC adaptions. It also compares various droop control strategies using MATLAB/Simulink simulations of an islanded MG. Section 5 proposes prospects for future research, and section 6 concludes the article.

2. Conventional Droop Control (CDC)

The underlying principle of CDC is to mimic the behaviour of conventional synchronous generators, allowing inverters to share load dynamically and proportionally without centralized communication. CDC is widely used and documented in literature [10, 18–21, 48–50]. When the CDC technique is applied to parallel inverters, it enables the adjustment of inverter frequency and power output based on the real time measured real and reactive power values. The theoretical analysis of power sharing among parallel inverters using CDC and the limitations of CDC in power sharing are discussed in the subsequent sections.

2.1. Theoretical Analysis of Power Sharing Using CDC

The analysis of CDC is based on the equivalent circuit of parallel connected inverters shown in Figure 3. The DG powers P_i and Q_i at the i[th] bus can be derived as [22, 51–54]

$$P_i = \frac{1}{Z_i}[(V_i V_0 \cos\delta_i - V_0^2)\cos\theta_i + V_i V_0 \sin\delta_i \sin\theta_i] \quad (1)$$

$$Q_i = \frac{1}{Z_i}[(V_i V_0 \cos\delta_i - V_0^2)\sin\theta_i + V_i V_0 \sin\delta_i \cos\theta_i] \quad (2)$$

Where, δ and θ are phase and impedance angles, respectively. The voltage at PCC, inverter output voltage and impedance magnitude are denoted by V_0,V_i and Z_i, respectively. Due to the significant inductive line impedance and the large inductor filter, the inverter output impedance in the CDC is regarded as purely inductive [50, 55]. Considering θ =90°, for MG with DG serving inductive load, the corresponding power outputs of the DG inverter are determined as follows:

$$P_i = \frac{V_i V_0}{X_i}\sin\delta_i \quad (3)$$

$$Q_i = \frac{V_i V_0 \cos\delta_i - V_0^2}{X_i} \quad (4)$$

In practical systems, the phase difference δ_i between bus voltages is small, leading to $\cos\delta_i = 1$ and, $\sin\delta_i = \delta_i$. Hence, power transfer Equations in (3) and (4) can be simplified to (5) and (6).

$$P_i = \frac{V_i V_0}{X_i}\delta_i \quad (5)$$

$$Q_i = \frac{V_0}{X_i}(V_i - V_0) \quad (6)$$

As indicated by Equations (5) and (6), the generation of reactive power is directly tied to the difference in voltage magnitude.

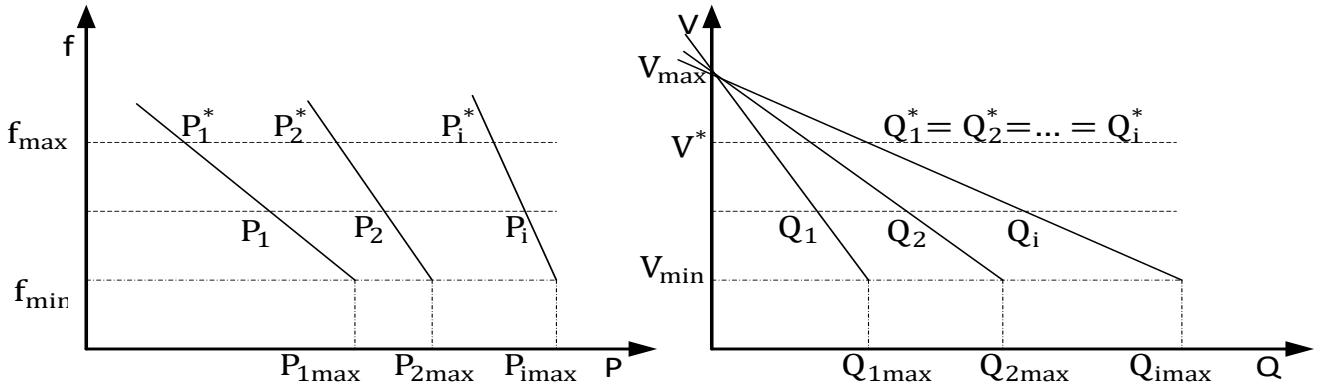

Fig. 4 Typical droop characteristics of CDC [17]

The real power output from the DG unit is entirely based on the phase angle difference. The control equations representing the relation between reactive power and voltage and actual power and frequency are:

$$f_i - f^* = -\mathrm{D}_{Pi}(P_i - P_i^*) \qquad (7)$$

$$V_i - V^* = -\mathrm{D}_{Qi}(Q_i - Q_i^*) \qquad (8)$$

(*) represent the nominal system values and ($_i$) the measured values of frequency, voltage and powers of ith parallel inverter. The P-f and Q-V characteristic slope is constant, and the P-f droop coefficient represents it. D_{Pi} and Q-V coefficient D_{Qi}. The selection of D_{Pi} and D_{Qi} significantly influences network stability, necessitating their careful and suitable design [56, 57]. The droop characteristics typical of the CDC are depicted in Figure 4 [17]. f_{min} represents the system's minimum permissible operating frequency, while V_{min} denotes the lowest acceptable output voltage amplitude.

The maximum power outputs of the DG unit's inverter are indicated by P_{max} and Q_{max}, respectively. The power shared by the DG unit will be increased by the Droop controller when there is a frequency drop and vice versa. When load reactive power demand is increased, the voltage of the AC system reduces and vice versa, and system AC voltage is maintained by modulation of reactive power [46]. This strategy can be effectively implemented in all MG's modes of operation. The droop coefficients are calculated according to the criteria for steady-state performance found in references [9, 19, 50]. The equations of droop coefficients can be written as follows:

$$D_P = \frac{\Delta f}{P_{max}} = \frac{f_{max} - f_{min}}{P_{max}} \qquad (9)$$

$$D_Q = \frac{\Delta V}{Q_{max}} = \frac{V_{max} - V_{min}}{Q_{max}} \qquad (10)$$

2.2. Problems with Precise Active and Reactive Power Sharing in CDC

Accurate power sharing is possible in CDC when the feeder impedance is predominantly inductive. However, CDC control presents several challenges for precise power sharing in various operational scenarios. These are discussed in depth in this section, supported by simulation results to provide deeper insights into the issues.

2.2.1. Power Coupling Due to Low X/R Ratio in LV Resistive MG

When employed in a power grid with predominantly inductive line impedances, the traditional CDC method for real and reactive power control neglects the line resistance, which may be sufficient under those circumstances. However, this approach becomes problematic in LV MGs, where feeder impedances are not predominantly inductive, and the resistance component (R) cannot be Ignored. This issue is particularly significant for DG units interfaced with power electronics, which lack a grid-side inductor or transformer, resulting in minimal output inductance. Under these conditions, even minor phase angle changes or voltage magnitude changes c significantly affect the real and reactive power flows [7, 24, 58]. If we assume a small power angle δ, we must modify Equations (1) and (2) accordingly.

$$P_i \approx \frac{V_i}{R}(V_i - V_0\cos(\delta_i)) \Rightarrow V_i - V_0 \approx \frac{RP}{V_i} \qquad (11)$$

$$Q_i \approx -\frac{V_i V_0 \sin(\delta_i)}{R} \Rightarrow \delta \approx -\frac{RQ}{V_i V_0} \qquad (12)$$

As a result, controlling the power flow using the conventional P–ω and Q–V droop methods will introduce a significant coupling between the real and reactive power flows, especially during transients and power sharing inaccuracies between the parallel connected inverters.

To better understand how system impedance influences power sharing, output active and reactive power behaviour across resistive impedance is depicted using polar coordinates in Figure 5. In this diagram, the radii represent the magnitudes of active and reactive power. In contrast, the polar angles represent the power angle δ, the phase difference between the inverter output voltage and the AC common bus voltage.

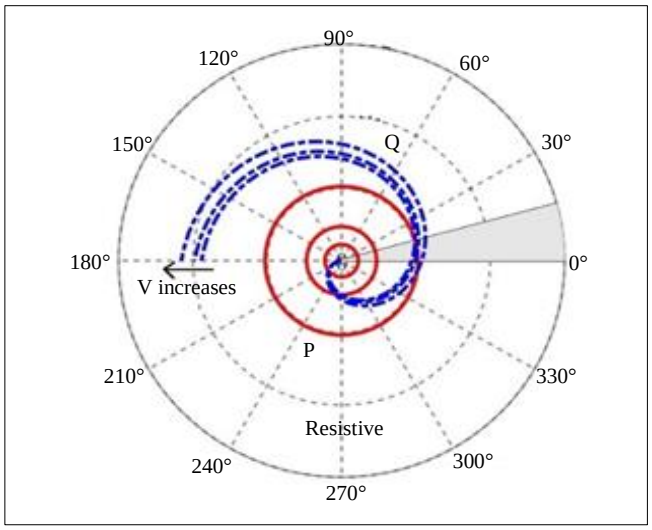

Fig. 5 Polar plot of the P/Q behaviours of parallel inverter with pure resistive impedance Solid line: P . Dashed line: Q

It is important to note that only the shaded areas in these figures are relevant in practical scenarios, as the power angle δ for each inverter is typically very small. In the case of pure resistive impedance, the behaviors of the active and reactive powers are inverse to the pure inductive impedances. Note that the inverter's delivered active and reactive powers still increase with the increase of V. However, here, the polar radius of the reactive power increases with the power angle δ, whereas the polar radius of the active power remains constant with δ variations.

2.2.2. Power Sharing Inaccuracy Due to Smaller Droop Coefficients

A small droop coefficient is essential to maintain system stability when managing frequency deviations within a narrow range. This approach ensures minimal frequency fluctuations, which is crucial for maintaining synchronous operation across the network. However, employing a small droop coefficient typically limits the effectiveness of active power sharing among distributed generators or units within the network [59–61]. This constraint is due to the reduced responsiveness of the power output to frequency changes, which is a core component of the droop control mechanism. Conversely, increasing the droop coefficient can significantly improve active power sharing.

With a larger droop coefficient, the system responds more dynamically to frequency changes, allowing for a more effective distribution of load changes among various power sources. This enhanced sharing capability helps balance load more efficiently and maintain operational reliability across the grid. However, the trade-off for better active power sharing is an increase in voltage deviations from their nominal values. A higher droop coefficient leads to greater output voltage sensitivity to frequency variations. This heightened sensitivity can result in larger voltage swings as the power output adjusts to maintain system frequency, potentially compromising voltage stability [59–61]. Such voltage fluctuations can affect the quality of power delivered to consumers and might require additional regulation or compensation mechanisms to manage. This balance between droop coefficient size, active power sharing, and voltage stability is critical in the design and operation of MG and other decentralized energy systems. Ensuring optimal droop settings requires carefully analysing the specific network characteristics and operational goals, often compromising stability, efficiency, and power quality.

2.2.3. Power Sharing Inaccuracy Due to Complex Line Impedance

The feeder line impedance is complex in several practical distribution grid applications [58]. Hence, neither the resistance nor the reactance of the line can be neglected in Equations (1) and (2). In feeders with complex impedance, there is a pronounced coupling between active and reactive power, which leads to inaccuracies in power sharing. This coupling complicates the decoupling process, making it more challenging to manage effectively [32]. Assuming that the phase differences δ between the inverter output voltage and the common bus voltage are minimal because the inverters are first synchronized by using the Phase-Locked Loop (PLL) module, then (3) and (4) can be simplified to

$$P_i \approx \frac{V_i}{Z_i}[(V_i - V_0)\cos\theta_i + V_i V_0 \sin\theta_i] \quad (13)$$

$$Q_i \approx \frac{V_i}{Z_i}[(V_i - V_0)\sin\theta_i + V_i V_0 \cos\theta_i] \quad (14)$$

It is seen from equations that the relationships between the output voltage and the delivered power are determined by the system impedance angle θ [62] According to Figure 6, both the active and the reactive powers increase their polar radius when the power angle δ increases. The active and imaginary power increases in a counter- clockwise direction when δ varies. The more inductive behavior of the complex impedance is emphasized to increase the amount of active power but decrease the reactive power. In contrast, the more resistive behavior of the complex impedance is emphasized to increase the amount of reactive power but decrease the active power. Because of this case, it can be concluded that the output power behavior of parallel inverters systems with complex impedance is entirely different from the other two conventional situations with inductive and resistive feeder impedances.

2.2.4. Inaccurate Power Sharing Due to Line Impedance Mismatches

The same voltage and frequency across the AC bus in an AC MG promotes precise active power sharing under P-ω control. However, challenges arise with Q-V droop control due to potential discrepancies in terminal voltages among parallel connected Inverter-based DG units because of line impedance-induced voltage drops.

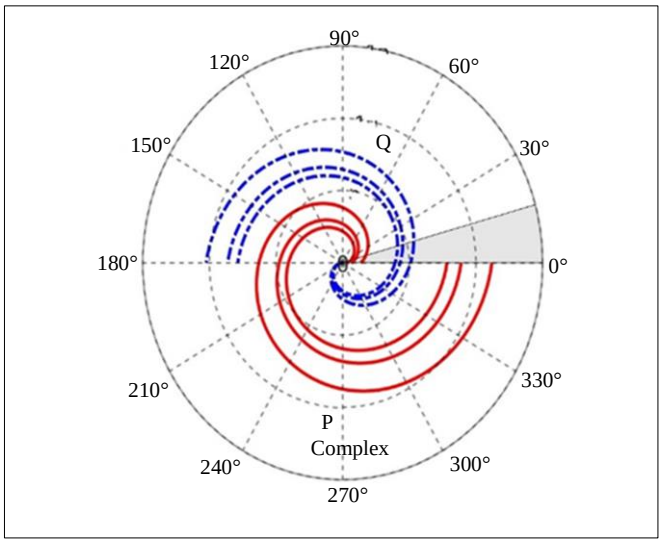

Fig. 6 Polar plot of the P/Q behaviours of parallel inverter with pure resistive impedance solid line: P . dashed line: Q

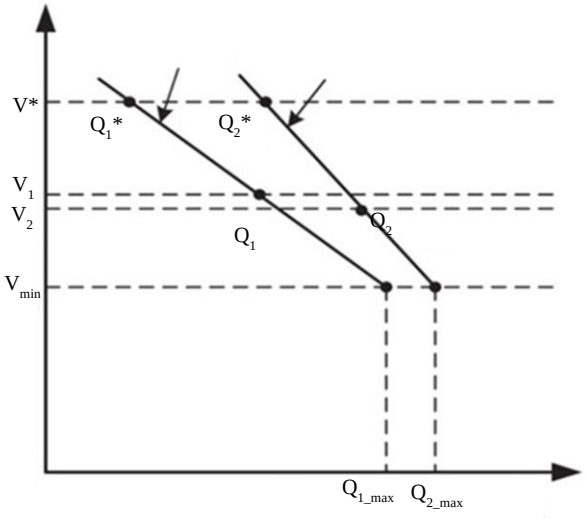

Fig. 7 Reactive power-sharing with CDC indicating errors caused by mismatched line impedances [58]

When the line impedances between the inverters and the point of common coupling are different, it could result in a considerable circulating current and low precision of power sharing among inverters. Consequently, the reactive power control delineated in specifications (2) and (10) may incur errors. As illustrated in Figure 7, variations in line impedance can lead to differential voltages across DG units, compromising power sharing accuracy[7, 24, 25, 58].

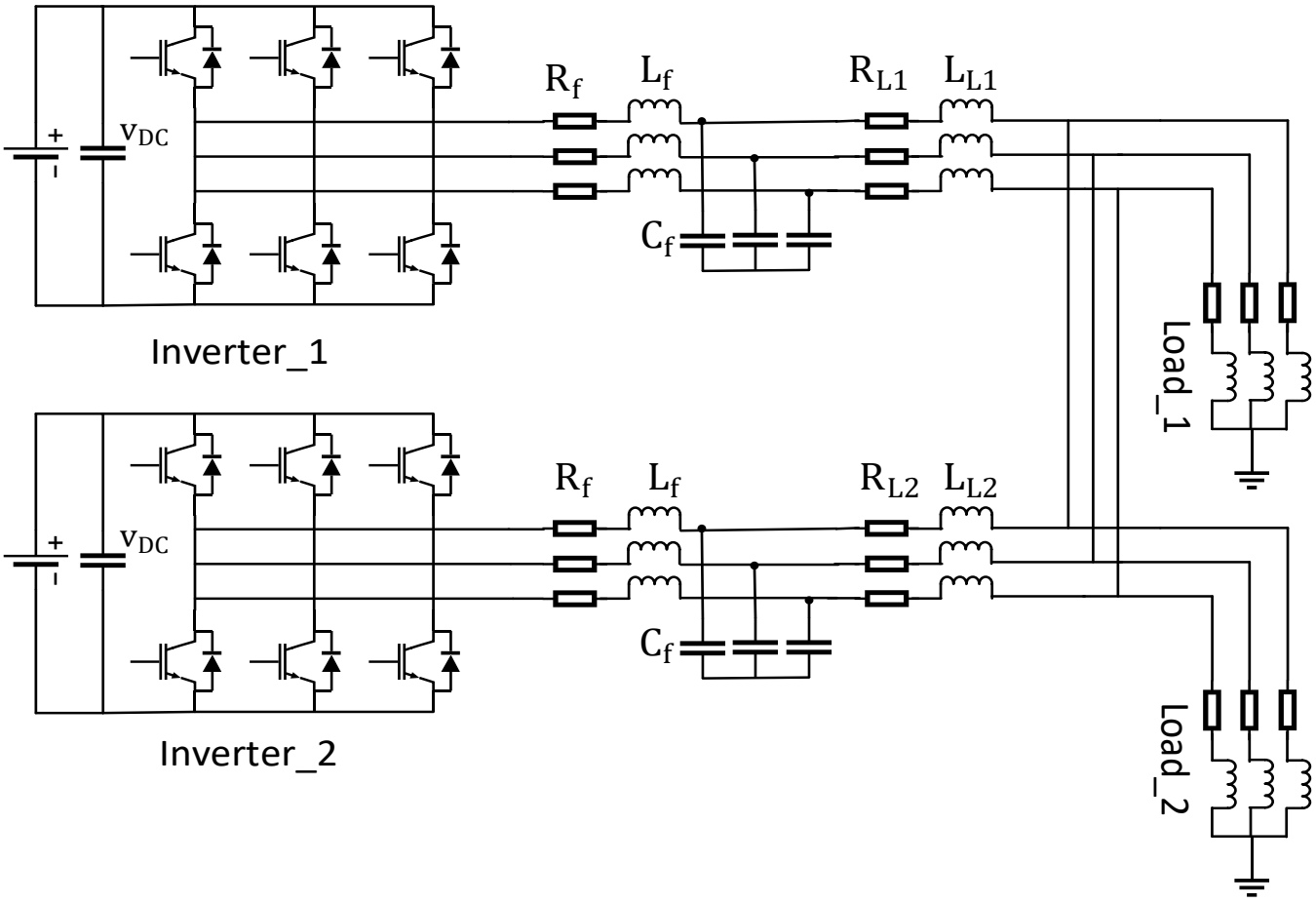

Fig. 8 MG model used for simulation

2.3. Simulation Studies

In this section, we use MATLAB/SIMULINK to analyse the performance of the CDC method under various operational scenarios, including inductive feeders with high X/R ratios, resistive feeders with low X/R ratios, mismatched line impedances, and conditions involving high droop gains. Figure 8 illustrates a circuit diagram of the system, which was modeled and simulated using MATLAB/Simulink. The simulation uses an MG configuration where two inverters of equal capacities are connected in parallel within an isolated islanded system. The MG model incorporates constant resistive and inductive loads, distribution lines with varying resistance-to-reactance ratios, and unequal output impedances among the inverters.

Each inverter employs a standard cascaded control architecture with an internal voltage controller and an internal current controller. The droop coefficients were designed to have an allowable voltage droop in the system of 5% and an allowable frequency droop of 0.5%. Details of the simulation parameters for the controllers are listed in Table 1 At $t = 0$, a load of 40 + j30 kVA is connected, and at $t = 1$ *s*, an identical load is added to evaluate the dynamic performance of the CDC.

Figures 9 to 11 illustrate the active and reactive power sharing under inductive, resistive, and complex (mixed inductive and resistive) feeder impedance conditions, respectively.

Table 1. Simulation parameters

	Parameter	Value
Inverter Filter	R_f	0.1Ω
	L_f	2.5mH
	C_f	50μF
System Parameters	Frequency (f)	50Hz
	Voltage	240V
Load 1	P+jQ kVA	40+j30 kVA
Load 2	P+jQ kVA	40+j30 kVA
CDC	D_P	1.57x 10^{-5}rad/W.s
	D_Q	2x10^{-4}V/VAr
CDC High Droop Gain	D_P	6.28x 10^{-5}rad/W.s
	D_Q	8x10^{-4}V/VAr
Line Parameters with mismatched and inductive line impedance	$R_{L1} + jX_{L1}$	0.004+ j0.2356 Ω
	$R_{L2} + jX_{L2}$	0.0045+ j0.1571 Ω
Line Parameters with mismatched and resistive line impedance	$R_{L1} + jX_{L1}$	1.1+ j0.2356 Ω
	$R_{L2} + jX_{L2}$	1.1 + j0.1571 Ω
Line Parameters with mismatched and complex line impedance	$R_{L1} + jX_{L1}$	0.2356+ j0.2356 Ω
	$R_{L2} + jX_{L2}$	0.1571 + j0.1571 Ω

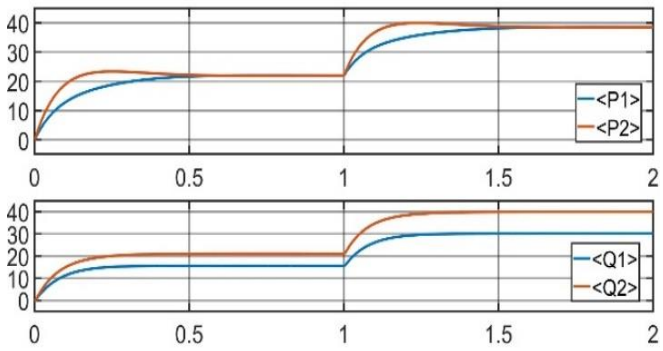

Fig. 9 Real and reactive power sharing of CDC with mismatched and inductive feeder impedance

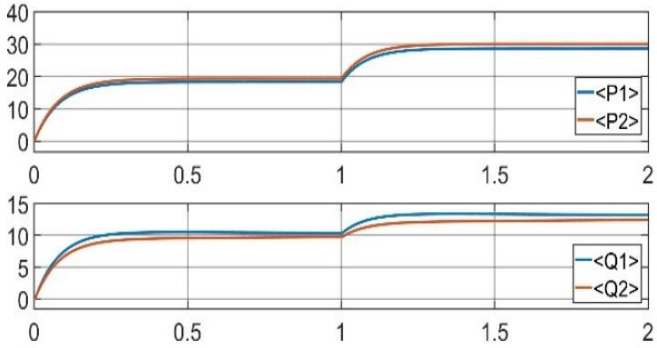

Fig. 10 Real and reactive power sharing of CDC with mismatched and resistive feeder impedance

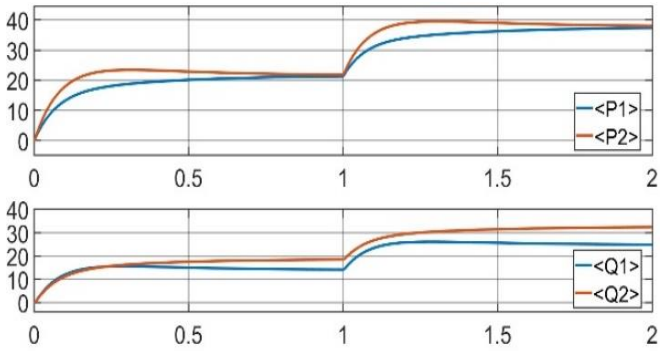

Fig. 11 Real and reactive power sharing of CDC with mismatched and complex feeder impedance

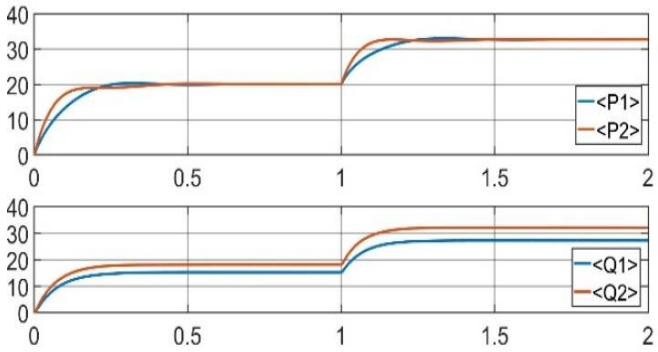

Fig. 12 Real and reactive power sharing of CDC with high droop gain inductive feeder impedance

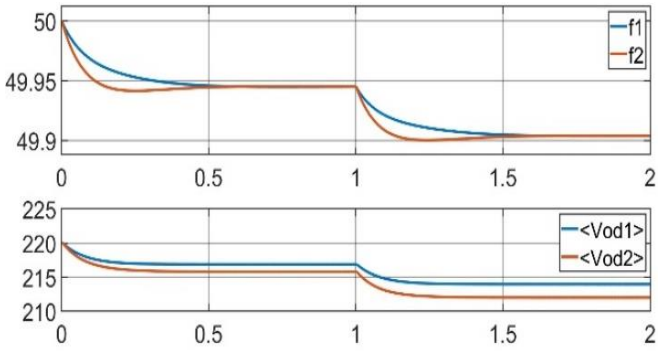

Fig. 13 Frequency and voltage response of CDC with mismatched and inductive feeder impedance with low droop gains

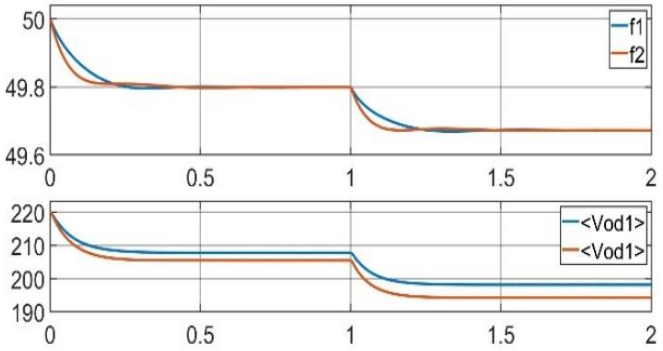

Fig. 14 Frequency and voltage response of CDC with mismatched and inductive feeder impedance with High droop gains

Figure 12 to 14 indicate the power sharing, voltage and frequency responses with high droop gains. Tables 2 and 3 provide quantitative metrics for real and reactive power sharing, including the percentage error compared to the ideal power-sharing scenario for parallel-connected inverters in an islanded MG under all the examined conditions.

The powers are measured at *t =0.9 sec* when the system attains the steady state condition. It can be seen from Table 2 that CDC accuracy in power sharing varies significantly depending on the type of feeder impedance and the chosen droop gain. With inductive line impedance, active power sharing is fairly accurate among the parallel inverters, with Inv 1 supplying 21.95 kW, 9.75% more than the ideal 20 kW, and Inv 2 providing 22.01 kW, representing a 10% increase.

However, the impact of mismatched line impedances on reactive power sharing is evident in Figure 9. Although both inverters have equal capacity, the terminal voltage discrepancies result in Inv 1 supplying 15.61 kVAr, which is 4.07% more than the ideal 15 kVAr, and Inv 2 providing 21.09 kVAr, representing a 40.6% increase. This imbalance highlights the significant influence of line impedance variations on reactive power distribution, even under identical inverter ratings. In MG, characterized by resistive and complex feeder impedances, the power coupling inherent in CDC methods leads to degraded power-sharing performance.

For a resistive MG, the sharing of active and reactive power significantly deviates from ideal values, as indicated by the high percentage of errors. In a complex impedance scenario, while active power allocation may improve, reactive power sharing remains notably imprecise. When comparing the inductive scenario to the inductive scenario with high droop gain, as shown in Figures 12, 13 and 14, it becomes clear that increasing the droop gain significantly improves active power-sharing accuracy.

Under purely inductive conditions, active power (P1 and P2) deviates from the ideal value by about 10%, while reactive power sharing-particularly Q2-shows a large 40.60% error. In contrast, when high droop gain is applied, the error in active power sharing is reduced to less than 1%, and the reactive power error, although still present, is also lowered for Q1. This enhanced precision, however, comes at a cost to power quality. Although low droop gains maintain voltage and frequency within 1–2% and 0.12% of their nominal values, higher gains cause voltage to drop by about 5–7% and frequency to deviate by around 0.4%.

Table 2. Real and reactive sharing comparison

MG Type	P_1(kW)	P_2(kW)	Q_1(kVAr)	Q_2(kVAr)	P_1(%error)	P_2(%error)	Q_1(%error)	Q_2(%error)
Inductive	21.95	22.01	15.61	21.09	9.75%	10.05%	4.07%	40.60%
Resistive	18.33	19.30	10.40	9.74	-8.35%	-3.50%	-30.67%	-35.07%
Complex	21.29	21.89	14.21	18.75	6.45%	9.45%	-5.27%	25.00%
High Droo Gain	20.06	20.08	15.27	18.16	0.30%	0.40%	1.80%	21.07%

Table 3. Voltage and frequency response comparison

MG Type	V_1 in Volts	f_1 in Hz	V_2 in Volts	f_2 in Hz	V_1 in Volts	f_1 in Hz	V_2 in Volts	f_2 in Hz
Inductive with Low Droop Gain	216.9	49.94	215.8	49.94	-1.41%	-0.12%	-1.91%	-0.12%
Inductive with High Droop Gain	207.8	49.8	205.6	49.8	-5.55%	-0.40%	-6.55%	-0.40%

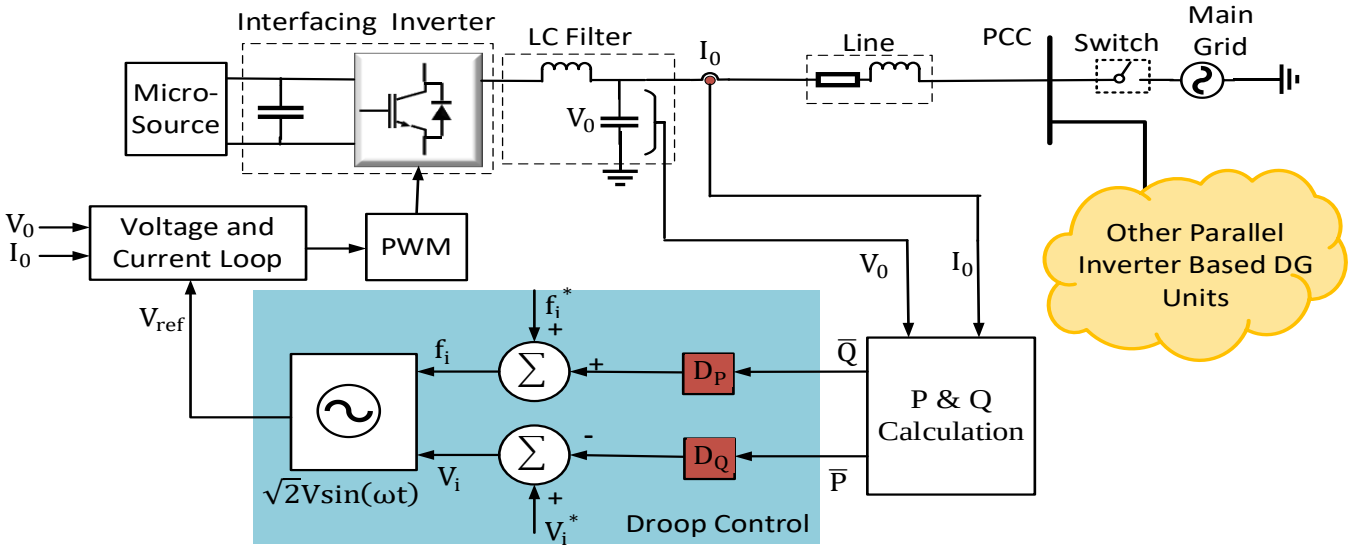

Fig. 15 Block diagram of reverse droop control

Thus, while higher droop gains can bolster power-sharing performance, they may simultaneously diminish overall power quality. The above discussion shows that the CDC struggles to maintain accurate power sharing under various feeder impedances and operating conditions. These challenges highlight the need for advanced droop control methods to handle complex, resistive, and mixed line conditions effectively. Such methods must offer better decoupling of power components, adapt to changing network parameters, and ensure both active and reactive power are shared with greater precision and stability. The following section explores these advanced methodologies and their potential to overcome the drawbacks of CDC.

3. Improvement in CDC for Accurate Power Sharing

The advanced droop control methods used to overcome CDC drawbacks, as discussed in an earlier section, are presented below. The synopsis of each method, including the improvement over CDC and the advantages and disadvantages, is presented in Table 4.

3.1. Improved CDC Control Under Resistive Feeder Impedance Condition

In resistive networks, the precision of active power sharing may be reduced when using CDC. To overcome this, before deploying CDC strategies, decoupling methods like linear transformation and the addition of virtual impedance are used [18, 24, 26, 63]. Moreover, reverse droop control strategies are often applied to attain equivalent active power sharing in environments with resistive feeder impedances [47, 50]. These are detailed in the following section.

3.1.1. Reverse Droop Control Method

Figure 15 depicts the conceptual representation of the reverse droop control method. The CDC is mainly suitable for feeders with pure inductive line impedances. In LVMG, the feeder impedance is predominantly resistive, causing inaccurate real power sharing among parallel inverters with CDC. The reverse droop control strategy is proposed in references [7, 20, 64] to address this issue. In this control, an increase in real power is associated with the voltage variation $(V_i - V_0)$ Moreover, an increase in reactive power is

associated with the change in power angle (δ) respectively [65].

$$P_i = \frac{V_0}{Z_i}(V_i - V_0) \quad (15)$$

$$Q_i = \frac{V_i V_0}{Z_i}\,\delta_i \quad (16)$$

Frequency regulation is achieved by managing the power angle by controlling reactive power consumption. Similarly, controlling the active power regulates the voltage as given in the control equations [62, 64, 66, 67] -

$$f_i - f^* = \mathrm{D}_{Pi}(Q_i - Q_i^*) \quad (17)$$

$$V_i - V^* = -\mathrm{D}_{Qi}(P_i - P_i^*) \quad (18)$$

This approach enhances control effectiveness in LV AC MGs characterized by predominately resistive transmission lines [62]. However, the performance of this method is heavily dependent upon the accurate knowledge of system parameters, which can considerably limit its practical deployment. Additionally, this strategy fails to address proper active load current distribution.

3.1.2. Virtual Frame Transformation Methods

A modification is suggested by the CDC to overcome the drawback for low X/R ratio lines [17] in the form of the Virtual Frame Transformation (VFT) method in the form of either P-Q or $\omega - V$ [24]. Virtual P-Q Frame Transformation [18, 26] is based on converting power components from the time domain into a virtual frame of reference. It is achieved using the orthogonal linear rotational transformation method, decouples active and reactive power, simplifying the control strategy. Under the assumption of mixed line impedance characteristics, the powers equations of ith DG inverter are expressed as:

$$P_i = \frac{V_0}{Z_i}\left[(V_i - V_0)\cos\theta_i + V_i\delta_i \sin\theta_i\right] \quad (19)$$

$$Q_i = \frac{V_0}{Z_i}\left[(V_i - V_0)\sin\theta_i - V_i\delta_i \cos\theta_i\right] \quad (20)$$

The decoupled powers are calculated as ,

$$\begin{bmatrix} P' \\ Q' \end{bmatrix} = T\begin{bmatrix} P \\ Q \end{bmatrix} = \begin{bmatrix} \sin\theta & -\cos\theta \\ \cos\theta & \sin\theta \end{bmatrix}\begin{bmatrix} P \\ Q \end{bmatrix} \quad (21)$$

$$P' = \frac{X}{Z}P - \frac{R}{Z}Q$$

$$Q' = \frac{R}{Z}P + \frac{X}{Z}Q$$

Like P-Q frame transformation, the virtual frequency/voltage frame ω'-V' can be expressed as [28–30]:

$$\begin{bmatrix} \omega' \\ V' \end{bmatrix} = \begin{bmatrix} \sin\theta & \cos\theta \\ -\cos\theta & \sin\theta \end{bmatrix}\begin{bmatrix} \omega \\ V \end{bmatrix} = T_{PQ}\begin{bmatrix} \omega \\ V \end{bmatrix} \quad (22)$$

$$\omega' = \frac{X}{Z}\omega - \frac{R}{Z}V \quad (23)$$

$$V' = \frac{R}{Z}\omega + \frac{X}{Z}V \quad (24)$$

These methods achieve PQ decoupling even in complex line impedance conditions. The transformed variables P',Q' and ω', V' are decoupled from each other. Generally, the precise R/X ratio may not be available; however, an estimated R/X ratio can often be adequate to apply the method [24, 68]

3.1.3. Virtual Impedance Based Methods

Introducing virtual impedance can adapt droop control for resistive lines. An enhanced droop control technique is designed by adding a virtual negative impedance with the CDC approach [31]. However, virtual impedance may lead to great voltage drop and harmonic amplification. Therefore, offsetting part of the line resistance with the virtual negative resistance can achieve equivalent performance with a smaller virtual impedance, improving voltage quality. In reference [7], a virtual inductor is proposed to estimate the voltage drops due to mismatched line impedance. This method improves the power sharing accuracy, specifically for LVMG with low X/R ratios. Specifically, the virtual inductance can effectively prevent the coupling between the real and reactive powers by introducing a predominantly inductive impedance, even in an LV network with resistive line impedances. The reactive power sharing algorithm functions by estimating the impedance voltage drops and significantly improves the reactive power control and sharing accuracy.

3.2. Improved CDC Control Under Complex and Unknown Feeder Impedance Condition

In a mixed resistive-inductive transmission line, adjusting the active power can impact the reactive power and vice versa, making independent control of each more challenging.

3.2.1. $(P-Q)\cdot f/(P+Q)\cdot V$ Method

Considering the impact of complex impedance, PQ decoupling can be achieved by the method suggested in [18, 19]. The control equations are given as

$$f_i - f^* = -\mathrm{D}_{Pi}\{(P_i - Q_i) - (P_i^* - Q_i^*)\} \quad (25)$$

$$V_i - V^* = -D_{Qi}\{(P_i + Q_i) - (P_i^* + Q_i^*)\} \quad (26)$$

Compared to the conventional droop method, this method offers efficient dynamic performance even in the case of MV MGs, where the transmission line R/X ratio is nearly one [68].

3.2.2. Adaptive Virtual Flux Droop (AVFD) Control Strategy

The AVFD control strategy proposed in [69] is a modification of the Virtua Flux Droop method to address issues arising from unequal line impedances, which can lead to inaccurate power sharing among DG units. It incorporates the idea of virtual impedance to mitigate the effects of mismatched line impedances, enabling accurate power sharing proportional to the ratings of the sources despite line

impedance mismatches. The control equations are given as [69].

$$\delta_i = \delta_i^* - D_{Pi}(P_i^* - P_i) - k_{ip}\int (P_i - P^*)dt \quad (27)$$

$$|\psi_i| = |\psi_i^*| - D_{Qi}(Q_i^* - Q_i) - k_{iq}\int (Q_i - Q^*)dt \quad (28)$$

k_{ip} and k_{iq} are compensatory coefficients for active and reactive powers, respectively, P^* and $Q^*$are active power and reactive power setpoints received from the Energy Management system of secondary control. The terms $k_{ip}\int (P_i - P^*)dt$ and $k_{iq}\int (Q_i - Q^*)dt$ account for long-term correction over real power imbalances and reactive power errors accumulated over time and $D_{Pi}(P_i^* - P_i)$ and $D_{Qi}(Q_i^* - Q_i)$ accounts for immediate droop response. The block diagram in Figure 16 illustrates the addition of integral control loops to manage active and reactive power in the system [69]. AVFD indirectly offsets the issues caused by mismatched line impedances using the compensatory terms in Equations (27) and (28), which mimic the impact of a theoretical virtual impedance. This technique ensures precise power distribution that aligns with the capacities of the different power sources.

3.2.3. Adaptive Droop with Frame Transformation

Reference [24] presents a novel adaptive droop with a frame transformation control strategy for DG inverters that allows for isolated and grid-tied operation. The strategy adapts to system changes and uses frame transformation to decouple active and reactive powers. DG inverter output powers P_i and Q_i are decoupled from the grid impedance and transformed into novel variables (P_{ci} and Q_{ci}) The droop control equations for phase angle control and voltage magnitude control are given as

$$\delta = -G_p(s)Z_g\left[(P_i - P_i^*)\sin\theta_g - (Q_i - Q_i^*)\cos\theta_g\right] \quad (29)$$

$$V = V^* - G_q(s)Z_g\left[(P_i - P_i^*)\cos\theta_g + (Q_i - Q_i^*)\sin\theta_g\right] \quad (30)$$

$G_p(s)$ and $G_q(s)$ represent the transfer functions that achieve decoupling via orthogonal frame transformation, explicitly designed for P-f and Q-V droop, respectively, with Z_g and θ_g denoting grid impedance and its phase angle. V^* stands as the amplitude voltage reference, adapting to grid and load dynamics. The controller design facilitates the dynamic modification of the DG inverter's output to align with shifts in power demand or other conditions, ensuring stability and efficiency. The transfer function of the controller is given as

$$G_p(s) = \frac{m_i + m_p s + m_d s^2}{s} \quad (31)$$

$$G_q(s) = \frac{n_i + n_p s}{s} \quad (32)$$

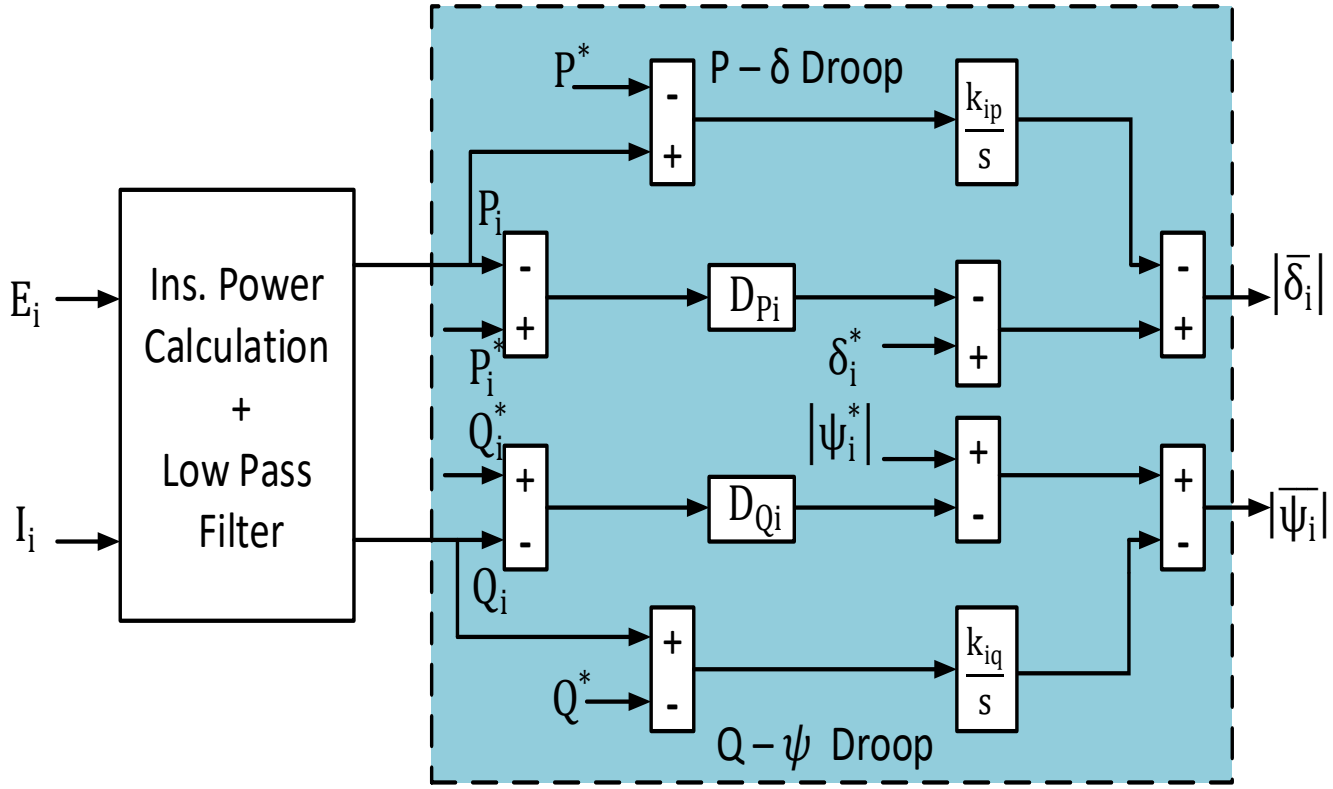

Fig. 16 Block diagram of adaptive virtual flux droop control

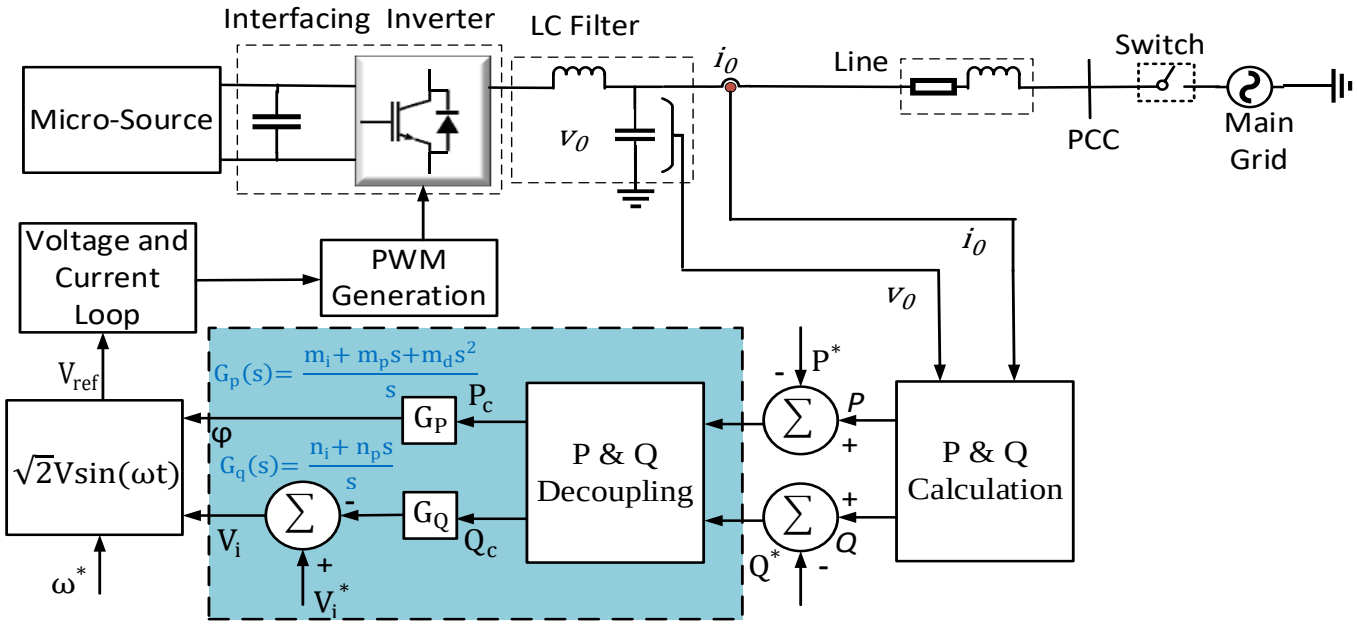

Fig. 17 Block diagram of adaptive FT based droop control

The conceptual representation of this method is depicted in Figure 17. The method described delivers precise and independent control over the injection of active and reactive power into the grid, optimizing performance without being influenced by the grid impedance magnitude or phase shifts.

3.3. Improved CDC Control Under Dynamic Loading Conditions

CDC offers inferior dynamic performance. The modified droop control strategies to improve the dynamic performance of the controller are discussed in the following section.

3.3.1. Adaptive P–δ Droop Control Strategies

In the Adaptive P–δ / Q-V Strategy, basic power-sharing is achieved using CDC, and supplementary adaptive control is used for enhanced stability and dynamic response [34]. Higher droop gains lead to larger changes in voltage or frequency for a given change in power, which can improve load sharing among multiple DG units. However, high droop gains can also make the system more sensitive to disturbances, potentially affecting system stability. The proposed supplementary controller addresses this challenge by ensuring system stability and power sharing accuracy even when high droop gains are used.

The control equations are given as.

$$\delta_i = \delta_i^* = -D_{Pi}\,(P_i - P_i^*) + \Delta\delta_i \qquad (33)$$

$$V_i - V_i^* = -D_{Qi}(Q_i^* - Q_i) + \Delta V_i \qquad (34)$$

$\Delta\delta_i$ and ΔV_i are the voltage magnitude and voltage angle correction by the adaptive controller. The block diagram of the control structure is depicted in Figure 18. The controller's parameters, such as gains and time constants, are optimized to ensure stability and to accommodate the range of operating conditions.

3.3.2. Derivative Term Based Adaptive Droop

In a relatively small AC MG, large load changes can be expected. The adaptive derivative term approach in [41, 42, 70] incorporates static and transient droop gains and aims to stabilise the low-frequency modes critical for power-sharing and improving the system's dynamic response. Transient droop gains, denoted as D'_P and D'_Q, are implemented to attenuate effectively damping fluctuations in power distribution among Distributed Generation (DG) units. The control equations are given by

$$f_i = f^* - D_{pi}(P_i - P_i^*) - D'_P\frac{dP_i}{dt} \qquad (35)$$

$$V_i - V^* = -D_{Qi}(Q_i - Q_i^*) - D'_Q\frac{dQ_i}{dt} \qquad (36)$$

Once the system has settled to its new equilibrium after transient, derivative terms no longer influence the control output. They are valid only for the system's dynamic behaviour; they are not used under steady-state conditions. Integrating a derivative term into the standard droop control effectively mitigates power fluctuations.

3.4. Improved CDC Control for Accurate Steady State Reactive Power Sharing

Unknown, unequal, complex line impedances cause inaccurate reactive power sharing among parallel DG units in CDC. Numerous CDC adaptations have been developed to address this problem and improve reactive power distribution among parallel inverters. These adaptations are detailed as follows:

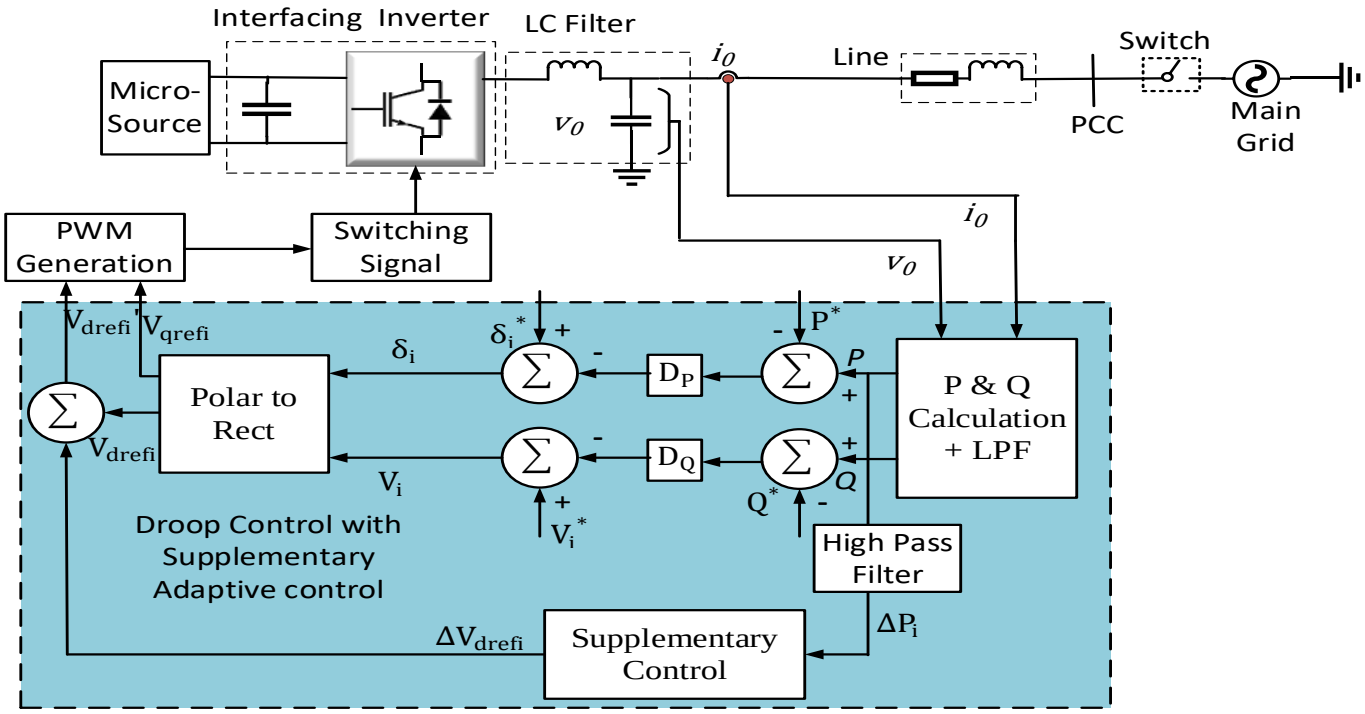

Fig. 18 Block diagram of adaptive P- δ / Q-V control

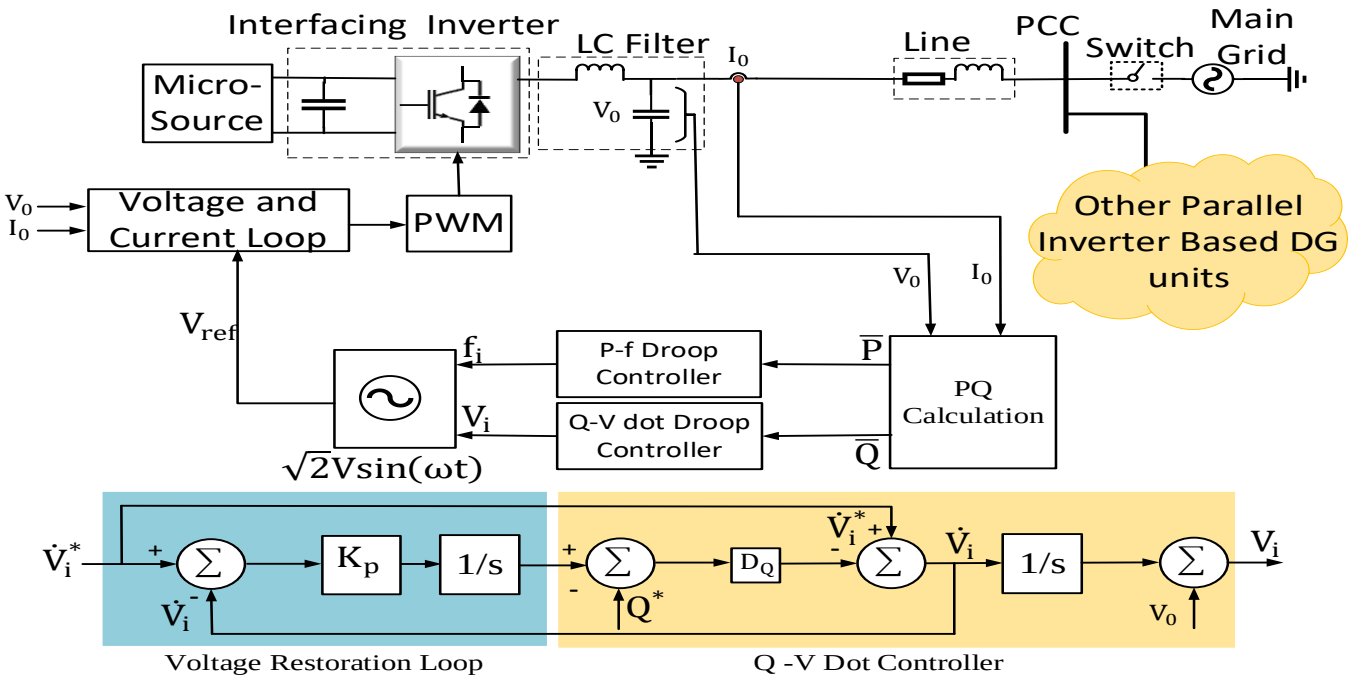

Fig. 19 Block diagram of P-f/ Q-V Dot method

3.4.1. The P-f / Q-V dot

The method proposed in [15, 36] is designed to make active power distribution among DG units in an MG independent of the line impedance. A key characteristic of this approach is that its effectiveness relies upon the system's initial conditions, which must be considered when implementing the control strategy. The control architecture for this method is depicted in Figure 19. The control equations are given by –

$$f_i = f_i^* - D_{pi}(P_i - P_i^*) \quad (37)$$

$$\dot{V}_i = \dot{V}_i^* - D_{Qi}(Q_i - Q_i^*) \quad (38)$$

$$V_i = \dot{V}_i^* + \int \dot{V}_i \, d\tau$$

Where, $\dot{V}_i^*$ is the nominal value of $\dot{V}_i$ which is set to 0 V/s. After any transient change, $\dot{V}_i$ is set to zero to ensure stable operation. Due to the differences in the restoration processes among various DGs [68], each DG might have a different set point for voltage or reactive power. Hence, power sharing accuracy is not completely improved in this method. A modified Voltage restoration loop is proposed in [71] to address the problem of setpoint deviation. Q − V˙ method's performance is degraded when the equivalent impedance is complex. Little attention has been paid to purely resistive cases compared to purely inducive cases [62, 72]. In [62], the output impedance of parallel DGs is shaped to be resistive, where the Q − V˙ droop equation is replaced by the P − V˙ droop control equation. The resistive output impedance makes the overall system more damped and automatically shares the harmonic current [72]. However, if the mismatch of feeder impedance is ignored, it will have great limitations in real applications. A virtual complex impedance-based P − V˙ droop method, which combines the advantages of both the virtual impedance-based method [23] and the Q − V˙ droop method [36], is proposed in [73] to solve the power-sharing problem of LVMG.

3.4.2. Virtual Impedance (VI) Method

Innovative and fast control loops to generate output impedance by simulating the effects of ideal (lossless) resistors or reactors, named virtual output impedance, are discussed in [74, 75]. The virtual impedance emulates the line impedance characteristics. A plethora of literature suggests improvements in CDC using the virtual output impedance method [18, 32, 63, 66, 74–79]. Figure 18 illustrates the schematic of the virtual impedance method. The reference voltage (V_{ref}) with fast VI droop control is calculated by deducting the VI voltage drop ($Z_V I_0$) from the reference voltage obtained from the droop controller (V^*) and given as:

$$V_{ref} = V^* - Z_V I_0 \quad (39)$$

In real time implementations, virtual inductive output impedance is realized by first calculating the time derivative of sensed fundamental output current, and then output voltage reference characteristics are drooped in proportion to that current. Figure 21 (a) and (b) depict the VI method's equivalent circuit and phasor diagram. The voltage drops due to virtual impedance and line impedance are $R_v\bar{I}$ and $jX_v\bar{I}$ and $R_l\bar{I}$ and $jX_l\bar{I}$ respectively. The DG output voltage is E, and the voltage at PCC is V_{PCC} making an angle of α and ϕ. $\bar{I}$ is the inverter output current. Usually, the virtual output impedance values will be higher than the line impedance [79].

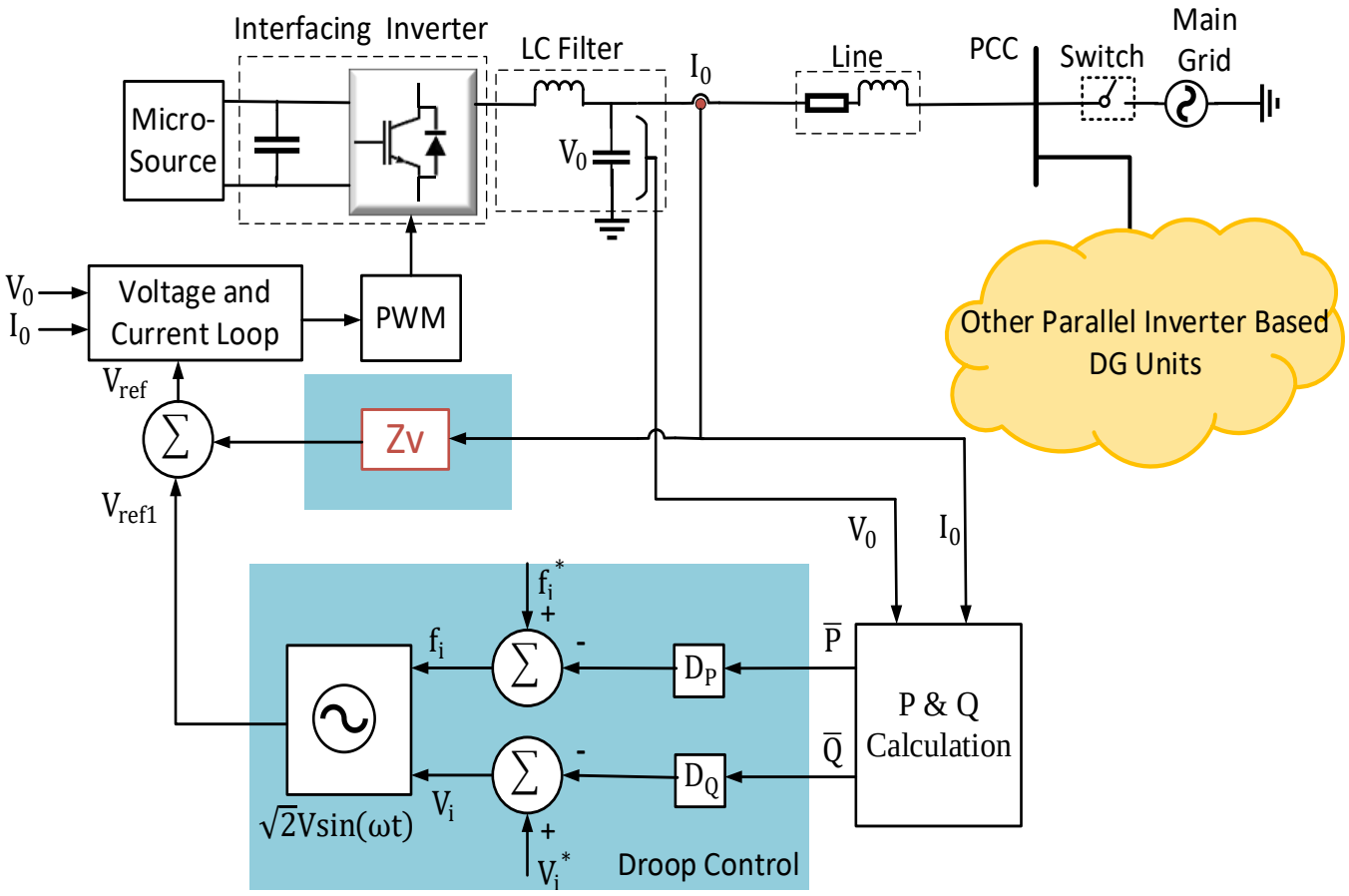

Fig. 20 Block diagram of virtual impedance droop control

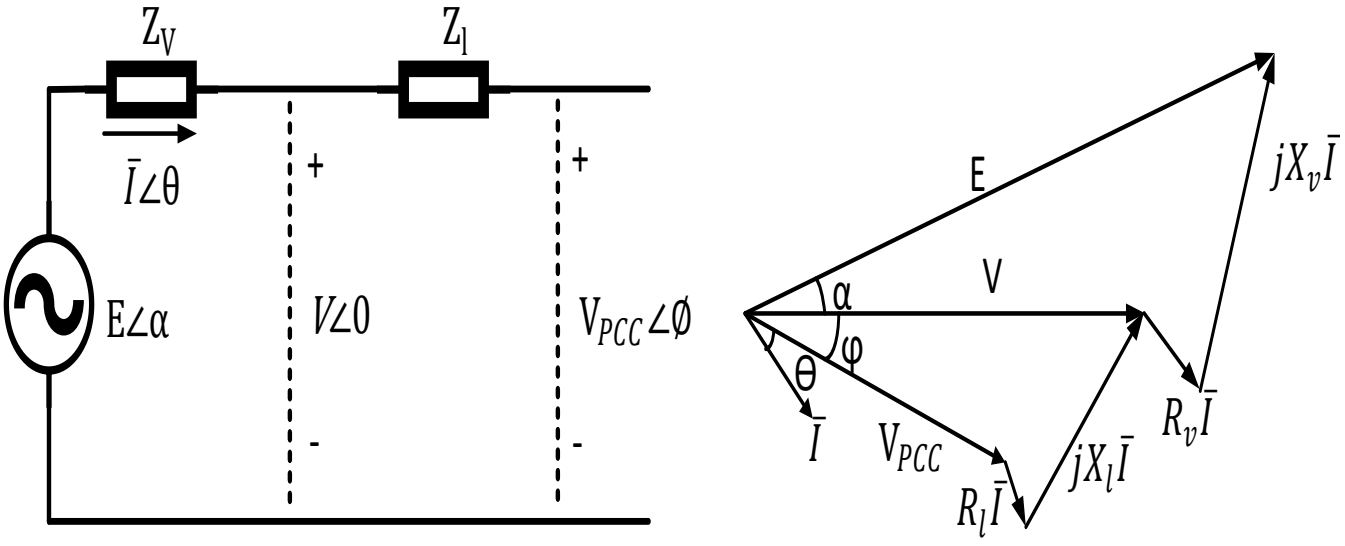

Fig. 21 Virtual impedance method (a) Equivalent circuit, and (b) Block diagram.

This is called the summation approach [27].

$$V_{drop1} = (Z_{l1} + Z_{V1})I_{l1} = V_{drop2} = (Z_{l2} + Z_{V2})I_{l2} \quad (40)$$

Where, Z_{V1} and Z_{V2} are output impedance of inverters and Z_{l1} and Z_{l2} are impedances to connecting lines to inverters 1 and 2, respectively. To determine the virtual impedance of inverter 1, which emulates the line impedance, the virtual impedance of inverter 2 is assumed to be zero. Z_{V2} can be fixed to zero if $Z_{l2} > Z_{l1}$. Then Z_{V1}can be calculated as

$$Z_{V1} = Z_{l1} - Z_{l2} \quad (41)$$

The above discussed summation method may reduce the virtual output impedance but improves reactive power sharing among grid inverters. Active and reactive powers can be decoupled by adequately adjusting the virtual impedance for either mainly inductive or restive distribution lines. Modifications have been reported in the Virtual output impedance strategy in literature for voltage unbalance compensation [80] to improve reactive power compensation and dynamic performance by active and reactive power coupling compensation [81] to achieve better reactive power and harmonic sharing [82].

3.4.3. Adaptive Virtual Impedance Based Droop Methods

The controller in [83] modifies the output impedance by tracking the power transfer difference between the inverter terminal and the PCC. The adaptive nature of the control allows for adjustment of the inverter output impedance autonomously. It provides improved damping and power-sharing performance across different MG types. Figure 22 shows the equivalent circuit of MG used for the analysis. The mismatched line impedances cause unequal voltage drops across two feeders ($\Delta V_{f1}, \Delta V_{f2}$), hence $\Delta V_{f1} \neq \Delta V_{f2}$. Voltage drop in MG feeder 1, ΔV_{f1} can be considered to be comprised of two components: voltage drop in the feeder ($\overline{\Delta V_{f1}}$) and mismtch voltege drop (δV_f) wherein the voltage drop in feeder 2 due to feeder impedance is only $\overline{\Delta V_{f1}}$

$$\Delta V_{f1} = \overline{\Delta V_{f1}} + \delta V_f \quad (42)$$

Table 4. Synopsis of modified CDC power sharing techniques

Control Method	Concept / Improves CDC on	Advantages	Disadvantages
Reverse Droop Control	• Adjusts power sharing in predominantly resistive MGs. • Problem Addressed: CDC's ineffectiveness in resistive environments with low X/R ratios.	• Tailored for resistive MGs	• Requires accurate system parameter knowledge • Poor Voltage and frequency regulation
Virtual P-Q Frame Structure Transformation	• Decouples P-Q via the virtual frame. • Problem Addressed: Strong P-Q coupling in mixed impedance lines causing inaccurate power sharing.	• Simplified control, decouples P and Q, enhancing power sharing accuracy.	• Variability in the virtual transformation angle can cause issues. • Implementation complexity; • requires virtual frame transformation.

Virtual ω-V Frame Structure Transformation	• Decouples P-Q via virtual frame • Problem Addressed: Addresses CDC's poor handling of impedance mismatches and power sharing inaccuracies.	• Facilitates independent control of P and Q, improving stability.	• Variations in virtual transformation angles can cause impedance mismatches and disrupt synchronization.
(P-Q). f/ (P+Q). V	• Incorporates line impedance characteristics for power sharing. Decouples P-Q in mixed impedance lines. • Problem Addressed: CDC's inability to effectively decouple P-Q in mixed impedance lines	• accurately shares power in MV MGs • Improves voltage regulation;	• Complex control strategy • Detailed line impedance knowledge is needed.
P-f / Q-V dot	• Introduces a voltage restoration loop to stabilize voltage over time. • Problem Addressed: Reactive power sharing challenges due to line impedance in CDC.	• Improves reactive power independence • Stabilizes voltage fluctuations	• Sensitive to initial system conditions • A steady-state solution may not exist • Easy to destabilize
Virtual Impedance Method	• Simulates line impedance for improved power sharing. • Problem Addressed: Addresses inaccurate reactive power sharing due to mismatched impedances.	• Enhanced stability • accurate power sharing • Harmonic power sharing is possible with its variants	• Increased control complexity, • challenges in transient response and voltage regulation.
Adaptive Virtual Impedance Based Droop Controller	• Modifies DG inverter output impedance by tracking power transfer differences. • Problem Addressed: Enhances damping and power-sharing performance.	• Improved power-sharing and system stability.	• Requires detailed knowledge of system parameters for optimal tuning.
Adaptive Virtual Flux Droop (AVFD) Control	• Adjusts virtual flux for power sharing, incorporating virtual impedance for mismatch compensation. • Problem Addressed: Addresses power sharing issues due to mismatched line impedances.	• Accurate power sharing proportional to DG ratings; • mitigates mismatch impacts	• Complex control strategy; potential challenges with rapid system changes.
Adaptive Droop Control based on Derivative Integral Terms	• Incorporates static and transient droop gains to stabilize low-frequency modes and improve system dynamics. • Problem Addressed: The static nature of traditional droop fails to compensate for fluctuating loads and varying line impedances.	• Stabilizes power sharing and enhances the dynamic response of the system.	• Complex control strategy, requiring tuning of derivative and integral terms. • The magnitude and phasor angle of output impedance are challenging to control because the virtual reactance is too dependent on voltage bandwidth.
Adaptive P–δ/V–Q Droop	• Uses CDC with supplementary adaptive control for enhanced stability and dynamic response. • Problem Addressed: Sensitivity to disturbances and instability due to high droop gains.	• Ensures system stability with high droop gains, responsive to rapid power changes.	• It necessitates additional control actions and has potential complexity in control implementation.

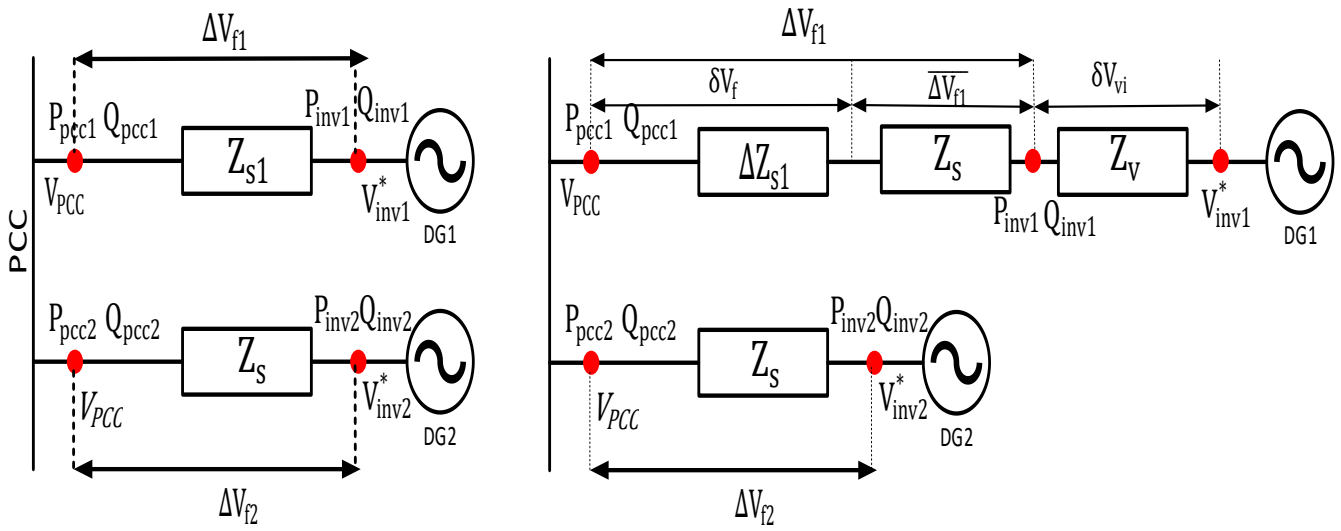

Fig. 22 Equivalent circuit of islanded MG with parallel inverters for adaptive virtual impedance droop control

Line impedance mismatches and their resulting unequal voltage drops are not considered in the voltage reference (V^*_{inv1}& V^*_{inv2}) by CDC. The voltage references are given as

$$V^*_{inv1} = V_{pcc} + \Delta V_{f1} + \delta V_f \tag{43}$$

$$V^*_{inv2} = V_{pcc} + \Delta V_{f2} \tag{44}$$

The VI control loop introduced in [83] will generate the reference voltage command such as δV_f^* cancels the effect of mismatched line impedance, $\delta V_f^* = \delta V_f$.

$$V^*_{inv1} + \delta V_f^* = V_{pcc} + \overline{\Delta V_{f1}} + \delta V_f \tag{45}$$

"Figure 10 depicts the graphical representation of the control method." The modified output impedance (Z_s) to counter the effect of mismatched line impedance is the sum of virtual impedance (Z_v) and the converter's inherent output impedance (Z_0) [83]:

$$\begin{aligned} Z_s &= Z_0 + Z_v \\ &= Z_0 + \frac{\omega_c}{s+\omega_c}\left[(P_{inv} - P_{pcc}) \times \left(K_{pp} + \frac{k_{ip}}{s}\right)\right. \\ &\quad + (Q_{inv} - Q_{pcc}) \\ &\quad \left. \times \left(K_{pv} + \frac{k_{iv}}{s}\right)\right] \end{aligned} \tag{46}$$

The difference between active and reactive powers at the inverter terminal and PCC is $\Delta P = (P_{inv} - P_{pcc})$ and $\Delta Q = (Q_{inv} - Q_{pcc})$. K_{pp}, k_{ip}, K_{pv}, k_{iv} are gains of controllers, ω_c is the cutoff frequency of the lowpass filter. This method improves damping and power-sharing performance across different MG DGs. Significant research has been devoted to implementing adaptive Virtual Impedance (VI) based strategies for enhancing the functionality of MGs. For example, an adaptive decentralized control technique based on virtual impedance proportional to DG output current to mitigate the effects of mismatched impedance is discussed in [84]. When the (R/X) ratio is low, CDC is applied, leading to equal sharing of real power but uneven distribution of reactive power. When the (R/X) ratio is high, the reverse droop control is employed, resulting in equal reactive power sharing at the expense of inaccurate real power distribution. In [85], an AVI control loop is proposed to improve power distribution in islanded MGs by addressing unbalance and harmonics. This method injects a small AC signal into each inverter's output voltage, achieving accurate real, reactive, and harmonic power sharing without needing a communication network or prior knowledge of system parameters. In [86], using the AVI method, a technique is proposed to improve the accuracy of reactive power distribution in isolated MGs. This approach adjusts Virtual Impedances (VIs) through communication to compensate for feeder impedance mismatches, ensuring accurate reactive power sharing despite communication delays and disruptions. Resistive, inductive and complex line impedances were utilized in [32, 37, 62] to improve the power sharing performance. It also alleviates the impact of feeder impedance mismatch; however, an accurate estimation of feeder impedance is required. The adaptive VI method [87] is proposed to achieve good power sharing performance, which works based on the difference between the active powers of DGs and average active powers. The method applies to parallel MGs only. In [88, 89], the AVI concept is used to get accurate reactive power sharing, which does not require prior knowledge of feeder impedances, but this method requires high bandwidth communication. The line current and PCC voltage are used in the feedback loop of the reference voltage to regulate the virtual impedance in [90, 91] to improve the power sharing accuracy with unbalanced and non-linear loads. It requires a complex neural network setup.

3.3.4. Additional Reactive Power Management Methods

The signal injection method proposed in [23, 92] effectively manages reactive power sharing and demonstrates resilience to changes in line impedances. In reference [23], each Distributed Generator (DG) injects a small AC voltage signal into the MG. Reactive power of DG unit, Q_i and boost signal m_{pi} are used to calculate the reference frequency f and the small real power p_q due to injected AC voltage adjusts the voltage reference of DG given by the equations

$$f_i = f_i^* - m_{qi}Q_i \quad (47)$$

$$V_i = V_i^* - n_{pi}p_q \quad (48)$$

However, this method suffers from the drawbacks of control complexity, higher losses and degraded power quality. Reference [25] introduces a novel method that improves the precision of reactive power sharing by utilizing small real power disturbances to estimate control errors in reactive power. Additionally, a slow integration term is added to the traditional Q-V droop control to rectify discrepancies in reactive power sharing.

However, this adjustment may compromise the accuracy of active power sharing. A decentralized, self-regulating control scheme is presented in Reference [93] to control reactive power and prevent its circulation among DG units, especially in the case of unequal feeder impedance. Reference [94] details a robust nonlinear distributed controller that stabilises powers, ensuring a quicker response under varying MG conditions such as three-phase short-circuit faults and load changes.

4. Comparative Evaluation

This section is divided into two parts, and the first section presents a comparative analysis of various advanced droop control methods based on various parameters such as the X/R ratio of line, system parameter sensitivity for control method, power sharing accuracy in mismatched line impedance scenarios, transient response, reactive power sharing precision and harmonic distortion management by the control. The second section performs a comparative assessment of various droop techniques, such as CDC, VI Droop, and Adaptive FT Droop, using the models of the controls developed in MATLAB/ Simulink.

Table 6. Performance Matrix

Control Method	Suitable for X/R Ratio	System Parameter Sensitivity	Suitable for Mismatched Line Impedances	Transient Response	Reactive Power Sharing Accuracy	Harmonic Distortion Management
CDC	High (Inductive)	Yes	No	Sluggish	Inaccurate	No
Reverse Droop Control	Low (Resistive)	Yes	No	Sluggish	Inaccurate	No
Virtual PQ Frame (VFT)	Low (Resistive)	Yes	No	Sluggish	Inaccurate	No
Virtual ω-V Frame	Low (Resistive)	Yes	No	Sluggish	Inaccurate	No
(P-Q). f/ (P+Q). V	All (Resistive + Inductive + Resistive Inductive)	Yes	No	Sluggish	Improved	No
P-f / Q-V dot	High (Inductive)	Yes	Yes	Sluggish	Accurate	No
Virtual Impedance Droop Control	All (Resistive + Inductive + Resistive Inductive)	No	Yes	Sluggish	Accurate	No
Adaptive Virtual Impedance Control	All (Resistive + Inductive + Resistive Inductive)	No	Yes	Sluggish	Accurate	No
Adaptive Virtual Flux Droop (AVFD)	All (Resistive + Inductive + Resistive Inductive)	Yes	Yes	Sluggish	Inaccurate	No
Adaptive Droop Control with Derivative Term	High (Inductive)	Yes	No	Improved	Inaccurate	No
Adaptive P–δ/V–Q Droop	High (Inductive)	Yes	No	Sluggish	Inaccurate	No
Adaptive Droop with Frame Transformation (ADFT)	All (Resistive + Inductive + Resistive Inductive)	Yes	No	Sluggish	Inaccurate	No

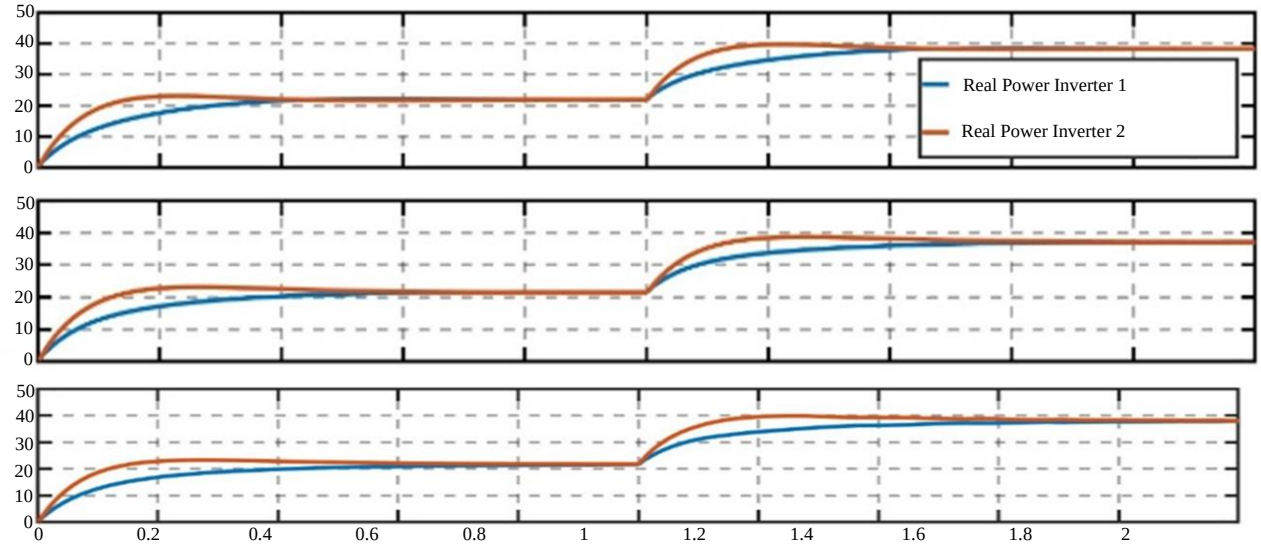

Fig. 23 Real Power Distribution among parallel inverters (a) CDC, (b) Virtual Impedance droop, and (c) Adaptive droop with frame transformation.

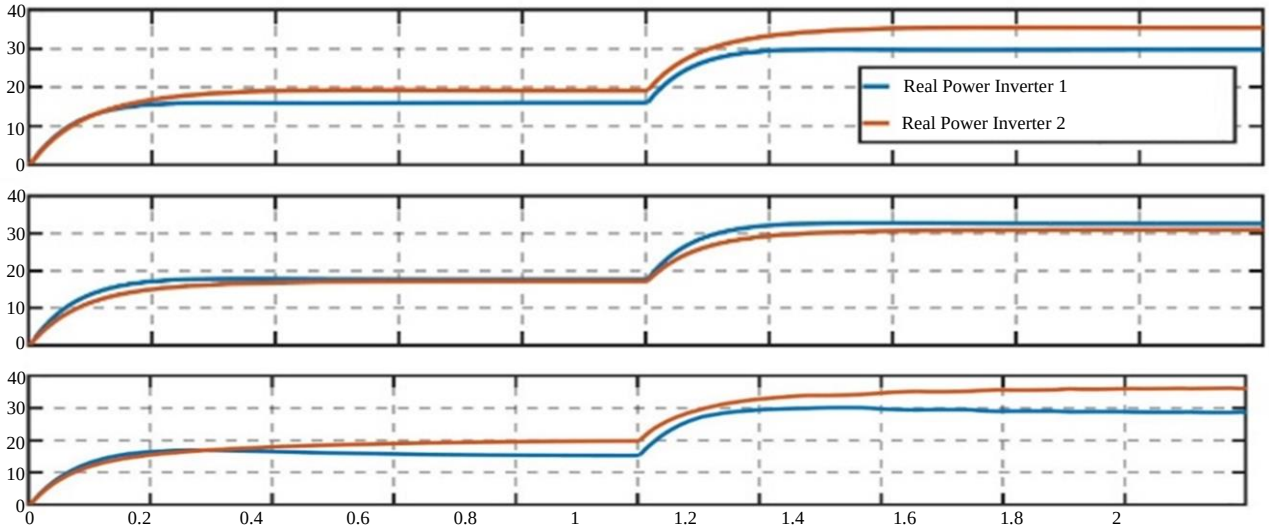

Fig. 24 Reactive power distribution among parallel inverters (a) CDC, (b) Virtual impedance droop, and (c) Adaptive droop with frame transformation.

4.1. Comparative Analysis Based on Key Performance Metrics

Lines with high R/X ratios, such as LV networks, are predominantly resistive, making power-sharing more challenging for CDC methods due to the strong coupling between active and reactive power. Conversely, lines with low R/X ratios, such as HV networks, are predominantly inductive, where CDC performs better as active and reactive power are naturally decoupled. For mixed R/X ratios, e.g., MV networks, advanced droop control methods are often necessary to address the complexities of power decoupling and impedance mismatches. Typical line impedance values for LV, MV, and HV lines are presented in Table 5, highlighting the differences in R/X ratios for different network types [95]. System parameter sensitivity indicates the reliance of a droop control method on accurate knowledge of system parameters such as line impedance, inverter output impedances and load conditions. High-sensitivity methods, such as CDC, require precise data for effective performance, while advanced methods like virtual impedance or adaptive droop reduce this dependency, offering more robust performance in dynamic or uncertain conditions. Transient response determines how quickly and smoothly a control method reacts to dynamic changes, such as load variations or faults. Methods with improved transient response stabilize the system faster and reduce oscillations than CDC. Reactive power sharing precision evaluates the ability of the control method to distribute reactive power proportionally among inverters, with advanced methods often achieving higher accuracy than traditional approaches.

Lastly, harmonic distortion management assesses the method's capability to mitigate or evenly share harmonics caused by nonlinear loads. Table 2 details the performance matrix of each method. CDC and its response stabilize the system faster and reduce oscillations compared to CDC. Reactive power sharing precision evaluates the ability of the control method to distribute reactive power proportionally among inverters, with advanced methods often achieving higher accuracy than traditional approaches. Lastly, harmonic distortion management assesses the method's capability to mitigate or evenly share harmonics caused by nonlinear loads. Table 2 details the performance matrix of each method. CDC and its basic variants, such as reverse droop and virtual frame transformations, perform well in specific conditions (e.g., high inductive or resistive X/R ratios) but show significant limitations in handling mismatched impedances, accurate reactive power sharing and transient response. Advanced methods like virtual impedance and adaptive virtual impedance controls demonstrate improved capabilities in managing mismatched line impedances and achieving accurate reactive power sharing, making them more robust for diverse line conditions. However, methods like adaptive droop with derivative terms show improved transient response but remain limited in reactive power sharing precision. Notably, harmonic distortion management is generally not addressed across most methods, highlighting a common limitation. This comparison underscores the need to choose droop control strategies based on specific network conditions and performance requirements.

4.2. Comparative Simulation Studies

This section performs a comparative assessment of various droop techniques, such as CDC, VI Droop, and Adaptive FT Droop. Details of the simulation parameters for the controllers are listed in Table 6. The model in Figure 8 is used for simulation. Simulation parameters are modified to suit advanced controllers like VI and Adaptive FT Droop. The virtual impedance is calculated using Equation (36) and (37) and comes out to be

$$R_{v2} + jX_{v2} = 0.02 + \text{j}0.0785\ \Omega$$

Table 5. Line impedance values

Line Type	R (Ω/km)	X (Ω/km)	R/X (pu)
LV	0.642	0.083	7.7
MV	0.161	0.190	0.85
HV	0.06	0.191	0.31

Table 6. Simulations parameters

	Parameter	Value
Inverter Filter	R_f	0.1Ω
	L_f	2.5mH
	C_f	50μF
Line Parameters	$R_{L1} + jX_{L1}$	0.1+ j0.2356 Ω
	$R_{L2} + jX_{L2}$	0.12 + j0.1571 Ω
System Parameters	Frequency (f)	50Hz
	Voltage	240V
Load 1	P+jQ kVA	40+j30 kVA
Load 2	P+jQ kVA	40+j30 kVA
CDC	D_P	1.57x 10^{-5}rad/W.s
	D_Q	2x10^{-4}V/VAr
Virtual Impedance Droop	$R_{v2} + jX_{v2}$	0.02 + j0.0785 Ω
Adaptive Droop with Frame Transformation	m_i, m_p, m_d	7x10^{-7} W/rad.s, 0.0015 W/rad, 0.0018 W.s/rad

Table 7. Real and reactive power sharing comparison

MG Type	P_1(kW)	P_2(kW)	Q_1(kVAr)	Q_2(kVAr)
CDC	21.95	22.01	15.61	21.09
VI	21.54	21.48	17.61	17.12
Adaptive FT	21.55	21.81	19.64	15.25

Table 8. Percentage error power sharing comparison

MG Type	P_1(% error)	P_2(% error)	Q_1(% error)	Q_2(% error)
CDC	9.75%	10.05%	4.07%	40.60%
VI	7.70%	7.40%	17.40%	14.13%
Adaptive FT	7.75%	9.05%	30.93%	1.67%

All the advanced strategies are tested using the same droop parameters and identical simulation setup with mismatched and inductive line impedance, as indicated in Table 6. At t = 0, the load of 40 +j30 kVA is connected, and at t = 1 s, an additional load of the same kVA rating is subsequently connected to simulate dynamic conditions in MG. Figure 23 depicts each strategy's real power sharing precision under simulation, whereas Figure 24 depicts reactive power distribution. The results in Tables 7 and 8 highlight the performance differences between CDC, VI, and Adaptive FT droop control methods in terms of real and reactive power-sharing accuracy.

All methods achieve relatively accurate real power sharing, with CDC showing slightly higher percentage errors (9.75% for P1 and 10.05% for P2) compared to VI (7.70% and 7.40%) and Adaptive FT (7.75% and 9.05%). VI and Adaptive FT methods provide comparable real power sharing improvements over CDC, reducing errors by approximately 2-3%.CDC exhibits significant errors in reactive power sharing, particularly for Q2 (40.60%), highlighting its inability to handle mismatched line impedances effectively.

VI improves reactive power sharing substantially, reducing Q2 errors to 14.13% while maintaining a moderate error for Q1 (17.40%). Adaptive FT demonstrates the lowest Q2 error (1.67%), indicating excellent performance in balancing reactive power among inverters. However, Q1

shows a relatively high error (30.93%), suggesting its accuracy is scenario-dependent. Despite reasonable accuracy for real power sharing, the CDC performs poorly in reactive power sharing, particularly under mismatched line conditions.

VI droop improves both real and reactive power sharing, making it a robust choice for systems requiring moderate precision across both metrics. Adaptive FT excels in reactive power sharing for Q2, significantly outperforming CDC and VI, but its higher Q1 error suggests further optimization may be required for specific scenarios. These results indicate that advanced droop methods significantly improve power-sharing performance compared to CDC, with each method offering unique strengths depending on the application requirements.

5. Critical Discussions and Future Aspects

In light of the comprehensive discussion on control tactics in the trailing sections for an AC MG, addressing the following topics could potentially resolve the identified challenges:

- Harmonic Distortion Management: While some droop control methods, like a variant of the Virtual Impedance method, offer potential for harmonic distortion management, there is a clear gap in integrated harmonic management across most methods. Hence, these methods need improvement.
- System Parameter Sensitivity: Many droop control strategies are highly sensitive to system parameters, necessitating accurate modeling and parameterization. Techniques that are less sensitive to system parameters are needed of the hour.
- Line Impedance Sensitivity: Line impedance mismatches affect power sharing accuracy in CDC. Robust methods sensitive to variations in line impedance and do not need extensive knowledge of system parameters could be highly beneficial.
- Reactive Power Sharing Accuracy: Reactive power sharing remains challenging in systems with mismatched line impedances. The controller must provide accurate reactive power sharing under all operating conditions and line characteristics.

6. Conclusion

This paper has presented a detailed classification from the point of view of applicability and a comprehensive overview of communication-free advanced droop control methods for power management in MGs. The comprehensive analysis leads to the following key findings:

- The analysis shows that each proposed control strategy for AC MGs is characterized by its distinctive features, advantages, and limitations, each catering to specific operational scenarios. For example, reverse droop control performs better in low X/R ratio scenarios but requires knowledge of accurate system parameters. Virtual impedance methods are superior in adaptability to line X/R ratio and mismatches but offer degraded performance for voltage regulation. Adaptive droop strategies provide better power sharing and regulation in dynamic conditions but at the cost of additional implementational complexity and computational burden.
- No single control strategy can fully address the limitations of the CDC regarding power sharing inaccuracies.
- Developing droop strategies that effectively manage the harmonics power sharing is imperative as the percentage of harmonic producing non-linear loads is increasing in power distribution systems.

References

[1] Fatih Birol, "*World Energy Outlook 2024*", International Energy Agency, Technical Report, 2024. [Publisher Link]

[2] Roger Lawrence, and S. Middlekauff, "The New Guy on the Block," *IEEE Industry Applications Magazine*, vol. 11, no. 1, pp. 54-59, 2005. [CrossRef] [Google Scholar] [Publisher Link]

[3] Sheng Su, YinHong Li, and XianZhong Duan, "Self-Organized Criticality of Power System Faults and Its Application in Adaptation to Extreme Climate," *Chinese Science Bulletin*, vol. 54, no. 7, pp. 1251-1259, 2009. [CrossRef] [Google Scholar] [Publisher Link]

[4] B. Satish, and S. Bhuvaneswari, "Control of Microgrid - A Review," *International Conference on Advances in Green Energy (ICAGE)*, Thiruvananthapuram, India, pp. 18-25, 2014. [CrossRef] [Google Scholar] [Publisher Link]

[5] Han Minxiao et al., "Transient Analysis and Control for Microgrid Stability Controller," *IEEE Grenoble Conference*, Grenoble, France, pp. 1-6, 2013. [CrossRef] [Google Scholar] [Publisher Link]

[6] Yao Zhang, and Hao Ma, "Theoretical and Experimental Investigation of Networked Control for Parallel Operation of Inverters," *IEEE Transactions on Industrial Electronics*, vol. 59, no. 4, pp. 1961-1970, 2012. [CrossRef] [Google Scholar] [Publisher Link]

[7] Yun Wei Li, and Ching-Nan Kao, "An Accurate Power Control Strategy for Power-Electronics-Interfaced Distributed Generation Units Operating in a Low-Voltage Multibus Microgrid," *IEEE Transactions on Power Electronics*, vol. 24, no. 12, pp. 2977-2988, 2009. [CrossRef] [Google Scholar] [Publisher Link]

[8] Qiang Fu et al., "Microgrid Generation Capacity Design with Renewables and Energy Storage Addressing Power Quality and Surety," *IEEE Transactions on Smart Grid*, vol. 3, no. 4, pp. 2019-2027, 2012. [CrossRef] [Google Scholar] [Publisher Link]

[9] Farid Katiraei, and M. Reza Iravani, "Power Management Strategies for a Microgrid with Multiple Distributed Generation Units," *IEEE Transactions on Power Systems*, vol. 21, no. 4, pp. 1821-1831, 2006. [CrossRef] [Google Scholar] [Publisher Link]

[10] Paolo Piagi, and Robert H. Lasseter, "Autonomous Control of Microgrids," *IEEE Power Engineering Society General Meeting*, Montreal, QC, Canada, 2006. [CrossRef] [Google Scholar] [Publisher Link]

[11] Z. Zeng, H. Yang, and R. Zhao, "Study on Small Signal Stability of Microgrids: A Review and a New Approach," *Renewable and Sustainable Energy Reviews*, vol. 15, no. 9, pp. 4818-4828, 2011. [CrossRef] [Google Scholar] [Publisher Link]

[12] Frede Blaabjerg et al., "Overview of Control and Grid Synchronization for Distributed Power Generation Systems," *IEEE Transactions on Industrial Electronics*, vol. 53, no. 5, pp. 1398-1409, 2006. [CrossRef] [Google Scholar] [Publisher Link]

[13] Robert H. Lasseter, and P. Paigi, "Microgrid: A Conceptual Solution," *IEEE 35th Annual Power Electronics Specialists Conference (IEEE Cat. No.04CH37551)*, Aachen, Germany, vol. 6, pp. 4285-4290, 2004. [CrossRef] [Google Scholar] [Publisher Link]

[14] Zhi Chen et al., "An Adaptive Virtual Resistor (AVR) Control Strategy for Low-Voltage Parallel Inverters," *IEEE Transactions on Power Electronics*, vol. 34, no. 1, pp. 863-876, 2019. [CrossRef] [Google Scholar] [Publisher Link]

[15] Chia-Tse Lee, Chia-Chi Chu, and Po-Tai Cheng, "A New Droop Control Method for the Autonomous Operation of Distributed Energy Resource Interface Converters," *IEEE Transactions on Power Electronics*, vol. 28, no. 4, pp. 1980-1993, 2013. [CrossRef] [Google Scholar] [Publisher Link]

[16] Qing-Chang Zhong, "Robust Droop Controller for Accurate Proportional Load Sharing Among Inverters Operated in Parallel," *IEEE Transactions on Industrial Electronics*, vol. 60, no. 4, pp. 1281-1290, 2013. [CrossRef] [Google Scholar] [Publisher Link]

[17] Daniel E. Olivares et al., "Trends in Microgrid Control," *IEEE Transactions on Smart Grid*, vol. 5, no. 4, pp. 1905-1919, 2014. [CrossRef] [Google Scholar] [Publisher Link]

[18] Karel De Brabandere et al., "A Voltage and Frequency Droop Control Method for Parallel Inverters," *IEEE Transactions on Power Electronics*, vol. 22, no. 4, pp. 1107-1115, 2007. [CrossRef] [Google Scholar] [Publisher Link]

[19] Yunwei Li, D. Mahinda Vilathgamuwa, and Poh Chiang Loh, "Design, Analysis, and Real-Time Testing of a Controller for Multibus Microgrid System," *IEEE Transactions on Power Electronics*, vol. 19, no. 5, pp. 1195-1204, 2004. [CrossRef] [Google Scholar] [Publisher Link]

[20] Charles Sao, and Peter W. Lehn, "Autonomous Load Sharing of Voltage Source Converters," *IEEE Transactions on Power Delivery*, vol. 20, no. 2, pp. 1009-1016, 2005. [CrossRef] [Google Scholar] [Publisher Link]

[21] Hassan Nikkhajoei, and Robert H. Lasseter, "Distributed Generation Interface to the CERTS Microgrid," *IEEE Transactions on Power Delivery*, vol. 24, no. 3, pp. 1598-1608, 2009. [CrossRef] [Google Scholar] [Publisher Link]

[22] A. Tuladhar et al., "Parallel Operation of Single Phase Inverter Modules with No Control Interconnections," *Proceedings of APEC 97 - Applied Power Electronics Conference*, Atlanta, GA, USA, vol. 1, pp. 94-100, 1997. [CrossRef] [Google Scholar] [Publisher Link]

[23] A. Tuladhar et al., "Control of Parallel Inverters in Distributed AC Power Systems with Consideration of Line Impedance Effect," *IEEE Transactions on Industry Applications*, vol. 36, no. 1, pp. 131-138, 2000. [CrossRef] [Google Scholar] [Publisher Link]

[24] Juan C. Vasquez et al., "Adaptive Droop Control Applied to Voltage-Source Inverters Operating in Grid-Connected and Islanded Modes," *IEEE Transactions on Industrial Electronics*, vol. 56, no. 10, pp. 4088-4096, 2009. [CrossRef] [Google Scholar] [Publisher Link]

[25] Jinwei He, and Yun Wei Li, "An Enhanced Microgrid Load Demand Sharing Strategy," *IEEE Transactions on Power Electronics*, vol. 27, no. 9, pp. 3984-3995, 2012. [CrossRef] [Google Scholar] [Publisher Link]

[26] Chia-Tse Lee et al., "Control Strategies for Distributed Energy Resources Interface Converters in the Low Voltage Microgrid," *IEEE Energy Conversion Congress and Exposition*, San Jose, CA, USA, pp. 2022-2029, 2009. [CrossRef] [Google Scholar] [Publisher Link]

[27] Christopher N. Rowe et al., "Implementing The Virtual Output Impedance Concept in a Three Phase System Utilising Cascaded PI Controllers in the Dq Rotating Reference Frame for Microgrid Inverter Control," *15th European Conference on Power Electronics and Applications (EPE)*, Lille, France, pp. 1-10, 2013. [CrossRef] [Google Scholar] [Publisher Link]

[28] Yan Li, and Yun Wei Li, "Decoupled Power Control for an Inverter Based Low Voltage Microgrid in Autonomous Operation," *IEEE 6th International Power Electronics and Motion Control Conference*, pp. 2490-2496, 2009. [CrossRef] [Google Scholar] [Publisher Link]

[29] Yan Li, and Yun Wei Li, "Power Management of Inverter Interfaced Autonomous Microgrid Based on Virtual Frequency-Voltage Frame," *IEEE Transactions on Smart Grid*, vol. 2, no. 1, pp. 30-40, 2011. [CrossRef] [Google Scholar] [Publisher Link]

[30] Yan Li, and Yun Wei Li, "Virtual Frequency-Voltage Frame Control of Inverter Based Low Voltage Microgrid," *IEEE Electrical Power and Energy Conference (EPEC)*, Montreal, QC, Canada, pp. 1-6, 2009. [CrossRef] [Google Scholar] [Publisher Link]

[31] Guolian Hou et al., "Virtual Negative Impedance Droop Method for Parallel Inverters in Microgrids," *IEEE 10th Conference on Industrial Electronics and Applications (ICIEA)*, Auckland, New Zealand, pp. 1009-1013, 2015. [CrossRef] [Google Scholar] [Publisher Link]

[32] Wei Yao et al., "Design and Analysis of the Droop Control Method for Parallel Inverters Considering the Impact of the Complex Impedance on the Power Sharing," *IEEE Transactions on Industrial Electronics*, vol. 58, no. 2, pp. 576-588, 2011. [CrossRef] [Google Scholar] [Publisher Link]

[33] Ahmed Moawwad, Vinod Khadkikar, and James L. Kirtley, "A New P-Q-V Droop Control Method for an Interline Photovoltaic (I-PV) Power System," *IEEE Transactions on Power Delivery*, vol. 28, no. 2, pp. 658-668, 2013. [CrossRef] [Google Scholar] [Publisher Link]

[34] Ritwik Majumder et al., "Improvement of Stability and Load Sharing in an Autonomous Microgrid Using Supplementary Droop Control Loop," *IEEE Transactions on Power Systems*, vol. 25, no. 2, pp. 796-808, 2010. [CrossRef] [Google Scholar] [Publisher Link]

[35] Hyun-Koo Kang, Seon-Ju Ahn, and Seung-Il Moon, "A New Method to Determine the Droop of Inverter-Based DGs," *IEEE Power and Energy Society General Meeting*, Calgary, AB, Canada, pp. 1-6, 2009. [CrossRef] [Google Scholar] [Publisher Link]

[36] Chia-Tse Lee, Chia-Chi Chu, and Po-Tai Cheng, "A New Droop Control Method for the Autonomous Operation of Distributed Energy Resource Interface Converters," *IEEE Energy Conversion Congress and Exposition*, Atlanta, GA, USA, pp. 702-709, 2010. [CrossRef] [Google Scholar] [Publisher Link]

[37] Christopher N. Rowe et al., "Arctan Power-Frequency Droop for Improved Microgrid Stability," *IEEE Transactions on Power Electronics*, vol. 28, no. 8, pp. 3747-3759, 2013. [CrossRef] [Google Scholar] [Publisher Link]

[38] Jiefeng Hu et al., "Virtual Flux Droop Method-A New Control Strategy of Inverters in Microgrids," *IEEE Transactions on Power Electronics*, vol. 29, no. 9, pp. 4704-4711, 2014. [CrossRef] [Google Scholar] [Publisher Link]

[39] E. Rokrok, and M.E.H. Golshan, "Adaptive Voltage Droop Scheme for Voltage Source Converters in an Islanded Multibus Microgrid," IET Generation, Transmission and Distribution, vol. 4, no. 5, pp. 562-578, 2010. [CrossRef] [Google Scholar] [Publisher Link]

[40] Jung-Won Kim, Hang-Seok Choi, and Bo Hyung Cho, "A Novel Droop Method for Converter Parallel Operation," *IEEE Transactions on Power Electronics*, vol. 17, no. 1, pp. 25-32, 2002. [CrossRef] [Google Scholar] [Publisher Link]

[41] Yasser Abdel-Rady Ibrahim Mohamed, and Ehab F. El-Saadany, "Adaptive Decentralized Droop Controller to Preserve Power Sharing Stability of Paralleled Inverters in Distributed Generation Microgrids," *IEEE Transactions on Power Electronics*, vol. 23, no. 6, pp. 2806-2816, 2008. [CrossRef] [Google Scholar] [Publisher Link]

[42] Jaehong Kim et al., "Mode Adaptive Droop Control with Virtual Output Impedances for an Inverter-Based Flexible AC Microgrid," *IEEE Transactions on Power Electronics*, vol. 26, no. 3, pp. 689-701, 2011. [CrossRef] [Google Scholar] [Publisher Link]

[43] Usman Bashir Tayab et al., "A Review of Droop Control Techniques For Microgrid," *Renewable and Sustainable Energy Reviews*, vol. 76, pp. 717-727, 2017. [CrossRef] [Google Scholar] [Publisher Link]

[44] Saroja Kanti Sahoo, Avinash Kumar Sinha, and N. Krishna Kishore, "Control Techniques in AC, DC, and Hybrid AC-DC Microgrid: A Review," *IEEE Journal of Emerging and Selected Topics in Power Electronics*, vol. 6, no. 2, pp. 738-759, 2018. [CrossRef] [Google Scholar] [Publisher Link]

[45] Jiefeng Hu et al., "Overview of Power Converter Control in Microgrids-Challenges, Advances, and Future Trends," *IEEE Transactions on Power Electronics*, vol. 37, no. 8, pp. 9907-9922, 2022. [CrossRef] [Google Scholar] [Publisher Link]

[46] Ajay Gupta, Suryanarayana Doolla, and Kishore Chatterjee, "Hybrid AC–DC Microgrid: Systematic Evaluation of Control Strategies," *IEEE Transactions on Smart Grid*, vol. 9, no. 4, pp. 3830-3843, 2018. [CrossRef] [Google Scholar] [Publisher Link]

[47] Kafeel Ahmed et al., "A Review on Primary and Secondary Controls of Inverter-Interfaced Microgrid," *Journal of Modern Power Systems and Clean Energy*, vol. 9, no. 5, pp. 969-985, 2021. [CrossRef] [Google Scholar] [Publisher Link]

[48] Farid Katiraei, M. Reza Iravani, and Peter W. Lehn, "Micro-Grid Autonomous Operation During and Subsequent to Islanding Process," *IEEE Power Engineering Society General Meeting*, Denver, CO, USA, vol. 2, 2004. [CrossRef] [Google Scholar] [Publisher Link]

[49] Fang Gao, and M. Reza Iravani, "A Control Strategy for a Distributed Generation Unit in Grid-Connected and Autonomous Modes of Operation," *IEEE Transactions on Power Delivery*, vol. 23, no. 2, pp. 850-859, 2008. [CrossRef] [Google Scholar] [Publisher Link]

[50] Mukul C. Chandorkar, Deepakraj M. Divan, and Ram Adapa, "Control of Parallel Connected Inverters in Standalone AC Supply Systems," *IEEE Transactions on Industry Applications*, vol. 29, no. 1, pp. 136-143, 1993. [CrossRef] [Google Scholar] [Publisher Link]

[51] Santanu K. Mishra, "Design-Oriented Analysis of Modern Active Droop-Controlled Power Supplies," *IEEE Transactions on Industrial Electronics*, vol. 56, no. 9, pp. 3704-3708, 2009. [CrossRef] [Google Scholar] [Publisher Link]

[52] Min Dai et al., "Power Flow Control of A Single Distributed Generation Unit with Nonlinear Local Load," *IEEE PES Power Systems Conference and Exposition*, New York, NY, USA, vol. 1, pp. 398-403, 2004. [CrossRef] [Google Scholar] [Publisher Link]

[53] Josep M. Guerrero, Lijun Hang, and Javier Uceda, "Control of Distributed Uninterruptible Power Supply Systems," *IEEE Transactions on Industrial Electronics*, vol. 55, no. 8, pp. 2845-2859, 2008. [CrossRef] [Google Scholar] [Publisher Link]

[54] Po-Tai Cheng et al., "A Cooperative Imbalance Compensation Method for Distributed-Generation Interface Converters," *IEEE Transactions on Industry Applications*, vol. 45, no. 2, pp. 805-815, 2009. [CrossRef] [Google Scholar] [Publisher Link]

[55] Xiaodan Bai, Hong Miao, and Chengbi Zeng, "Improved Droop Control Strategy for Reactive Power Sharing of Parallel Inverters In Low-Voltage Microgrid," *IEEE Innovative Smart Grid Technologies - Asia (ISGT Asia)*, Chengdu, China, pp. 2538-2543, 2019. [CrossRef] [Google Scholar] [Publisher Link]

[56] Ernane Antônio Alves Coelho, Porfrio Cabaleiro Cortizo, and Pedro F. Donoso Garcia, "Small-Signal Stability for Parallel-Connected Inverters in Stand-Alone AC Supply Systems," *IEEE Transactions on Industry Applications*, vol. 38, no. 2, pp. 533-542, 2002. [CrossRef] [Google Scholar] [Publisher Link]

[57] Nagaraju Pogaku, Milan Prodanovic, and Timothy C. Green, "Modeling, Analysis and Testing of Autonomous Operation of an Inverter-Based Microgrid," *IEEE Transactions on Power Electronics*, vol. 22, no. 2, pp. 613-625, 2007. [CrossRef] [Google Scholar] [Publisher Link]

[58] Yunwei Ryan Li, Farzam Nejabatkhah, and Hao Tian, *Smart Hybrid AC/DC Microgrids: Power Management, Energy Management, and Power Quality Control*, John Wiley & Sons, Ltd, 2022. [Google Scholar] [Publisher Link]

[59] Yasser Abdel-Rady I. Mohamed, and Amr A. Radwan, "Hierarchical Control System for Robust Microgrid Operation and Seamless Mode Transfer in Active Distribution Systems," *IEEE Transactions on Smart Grid*, vol. 2, no. 2, pp. 352-362, 2011. [CrossRef] [Google Scholar] [Publisher Link]

[60] Alireza Kahrobaeian, and Yasser Abdel-Rady Ibrahim Mohamed, "Networked-Based Hybrid Distributed Power Sharing and Control for Islanded Microgrid Systems," *IEEE Transactions on Power Electronics*, vol. 30, no. 2, pp. 603-617, 2015. [CrossRef] [Google Scholar] [Publisher Link]

[61] Inam Ullah Nutkani et al., "Linear Decentralized Power Sharing Schemes for Economic Operation of AC Microgrids," *IEEE Transactions on Industrial Electronics*, vol. 63, no. 1, pp. 225-234, 2016. [CrossRef] [Google Scholar] [Publisher Link]

[62] Josep M. Guerrero et al., "Decentralized Control for Parallel Operation of Distributed Generation Inverters Using Resistive Output Impedance," *IEEE Transactions on Industrial Electronics*, vol. 54, no. 2, pp. 994-1004, 2007. [CrossRef] [Google Scholar] [Publisher Link]

[63] Josep M. Guerrero et al., "Control Strategy for Flexible Microgrid Based on Parallel Line-Interactive UPS Systems," *IEEE Transactions on Industrial Electronics*, vol. 56, no. 3, pp. 726-736, 2009. [CrossRef] [Google Scholar] [Publisher Link]

[64] Xiaoxiao Yu et al., "Control of Parallel-Connected Power Converters for Low-Voltage Microgrid-Part I: A Hybrid Control Architecture," *IEEE Transactions on Power Electronics*, vol. 25, no. 12, pp. 2962-2970, 2010. [CrossRef] [Google Scholar] [Publisher Link]

[65] Dan Wu, Fen Tang, J.C. Vasquez, and J.M. Guerrero, "Control and Analysis of Droop and Reverse Droop Controllers for Distributed Generations," *IEEE 11th International Multi-Conference on Systems, Signals and Devices (SSD14)*, Barcelona, Spain, 2014, pp. 1-5, 2014. [CrossRef] [Google Scholar] [Publisher Link]

[66] Josep Maria Guerrero et al., "Output Impedance Design of Parallel-Connected UPS Inverters with Wireless Load-Sharing Control," *IEEE Transactions on Industrial Electronics*, vol. 52, no. 4, pp. 1126-1135, 2005. [CrossRef] [Google Scholar] [Publisher Link]

[67] Charles K. Sao, and Peter W. Lehn, "Control and Power Management of Converter Fed Microgrids," *IEEE Transactions on Power Systems*, vol. 23, no. 3, pp. 1088-1098, 2008. [CrossRef] [Google Scholar] [Publisher Link]

[68] Hua Han et al., "Review of Power Sharing Control Strategies for Islanding Operation of AC Microgrids," *IEEE Transactions on Smart Grid*, vol. 7, no. 1, pp. 200-215, 2016. [CrossRef] [Google Scholar] [Publisher Link]

[69] Saheb Khanabdal et al., "Adaptive Virtual Flux Droop Control Based on Virtual Impedance in Islanded AC Microgrids," *IEEE Journal of Emerging and Selected Topics in Power Electronics*, vol. 10, no. 1, pp. 1095-1107, 2022. [CrossRef] [Google Scholar] [Publisher Link]

[70] II-Yop Chung et al., :Control Methods of Inverter-Interfaced Distributed Generators in a Microgrid System," *IEEE Transactions on Industry Applications*, vol. 46, no. 3, pp. 1078-1088, 2010. [CrossRef] [Google Scholar] [Publisher Link]

[71] Jiuyang Zhou, and Po-Tai Cheng, "A Modified Q-V̇ Droop Control for Accurate Reactive Power Sharing in Distributed Generation Microgrid," *IEEE Transactions on Industry Applications*, vol. 55, no. 4, pp. 4100-4109, 2019. [CrossRef] [Google Scholar] [Publisher Link]

[72] Tine L. Vandoorn et al., "Automatic Power-Sharing Modification of P/V Droop Controllers in Low-Voltage Resistive Microgrids," *IEEE Transactions on Power Delivery*, vol. 27, no. 4, pp. 2318-2325, 2012. [CrossRef] [Google Scholar] [Publisher Link]

[73] Jianbo Chen et al., "A Virtual Complex Impedance Based P-V̇ Droop Method for Parallel-Connected Inverters in Low-Voltage AC Microgrids," *IEEE Transactions on Industrial Informatics*, vol. 17, no. 3, pp. 1763-1773, 2021. [CrossRef] [Google Scholar] [Publisher Link]

[74] Alfred Engler, "Control of Parallel Operating Battery Inverters," *Photovoltaic Hybrid Power Systems Conference*, Aix-en-Provence, pp. 1-4, 2000. [Google Scholar]

[75] S.J. Chiang, Chih-Ying Yen, and Kuo-Tsai Chang, "A Multimodule Parallelable Series-Connected PWM Voltage Regulator," *IEEE Transactions on Industrial Electronics*, vol. 48, no. 3, pp. 506-516, 2001. [CrossRef] [Google Scholar] [Publisher Link]

[76] Josep M. Guerrero et al., "Hierarchical Control of Droop-Controlled AC and DC Microgrids-A General Approach Toward Standardization," *IEEE Transactions on Industrial Electronics*, vol. 58, no. 1, pp. 158-172, 2011. [CrossRef] [Google Scholar] [Publisher Link]

[77] Josep Maria Guerrero et al., "Wireless-Control Strategy for Parallel Operation of Distributed-Generation Inverters," *IEEE Transactions on Industrial Electronics*, vol. 53, no. 5, pp. 1461-1470, 2006. [CrossRef] [Google Scholar] [Publisher Link]

[78] Josep M. Guerrero et al., "Advanced Control Architectures for Intelligent Microgrids-Part I: Decentralized and Hierarchical Control," *IEEE Transactions on Industrial Electronics*, vol. 60, no. 4, pp. 1254-1262, 2013. [CrossRef] [Google Scholar] [Publisher Link]

[79] Alexander Micallef et al., "Reactive Power Sharing and Voltage Harmonic Distortion Compensation of Droop Controlled Single Phase Islanded Microgrids," *IEEE Transactions on Smart Grid*, vol. 5, no. 3, pp. 1149-1158, 2014. [CrossRef] [Google Scholar] [Publisher Link]

[80] Mehdi Savaghebi et al., "Autonomous Voltage Unbalance Compensation in an Islanded Droop-Controlled Microgrid," *IEEE Transactions on Industrial Electronics*, vol. 60, no. 4, pp. 1390-1402, 2013. [CrossRef] [Google Scholar] [Publisher Link]

[81] Zishun Peng et al., "Droop Control Strategy Incorporating Coupling Compensation and Virtual Impedance for Microgrid Application," *IEEE Transactions on Energy Conversion*, vol. 34, no. 277-291, 2019. [CrossRef] [Google Scholar] [Publisher Link]

[82] Allal M. Bouzid et al., "A Survey on Control of Electric Power Distributed Generation Systems for Microgrid Applications," *Renewable and Sustainable Energy Reviews*, vol. 44, pp.751-766, 2015. [CrossRef] [Google Scholar] [Publisher Link]

[83] Moudud Ahmed et al., "Adaptive Virtual Impedance Controller for Parallel and Radial Microgrids With Varying X/R Ratios," *IEEE Transactions on Sustainable Energy*, vol. 13, no. 2, pp. 830-843, 2022. [CrossRef] [Google Scholar] [Publisher Link]

[84] A.S. Vijay et al., "An Adaptive Virtual Impedance Control for Improving Power Sharing among Inverters in Islanded AC Microgrids," *IEEE Transactions on Smart Grid*, vol. 12, no. 4, pp. 2991-3003, 2021. [CrossRef] [Google Scholar] [Publisher Link]

[85] Baojin Liu et al., "An Adaptive Virtual Impedance Control Scheme Based on Small-AC-Signal Injection for Unbalanced and Harmonic Power Sharing in Islanded Microgrids," *IEEE Transactions on Power Electronics*, vol. 34, no. 12, pp. 12333-12355, 2019. [CrossRef] [Google Scholar] [Publisher Link]

[86] Hisham Mahmood, Dennis Michaelson, and Jin Jiang, "Accurate Reactive Power Sharing in an Islanded Microgrid Using Adaptive Virtual Impedances," *IEEE Transactions on Power Electronics*, vol. 30, no. 3, pp. 1605-1617, 2015. [CrossRef] [Google Scholar] [Publisher Link]

[87] Baoze Wei et al., "DAVIC: A New Distributed Adaptive Virtual Impedance Control for Parallel-Connected Voltage Source Inverters in Modular UPS System," *IEEE Transactions on Power Electronics*, vol. 34, no. 6, pp. 5953-5968, 2019. [CrossRef] [Google Scholar] [Publisher Link]

[88] Tuan V. Hoang, and Hong-Hee Lee, "An Adaptive Virtual Impedance Control Scheme to Eliminate the Reactive-Power-Sharing Errors in an Islanding Meshed Microgrid," *IEEE Journal of Emerging and Selected Topics in Power Electronics*, vol. 6, no. 2, pp. 966-976, 2018. [CrossRef] [Google Scholar] [Publisher Link]

[89] Mohsen Eskandari et al., "A Control System for Stable Operation of Autonomous Networked Microgrids," *IEEE Transactions on Power Delivery*, vol. 35, no. 4, pp. 1633-1647, 2020. [CrossRef] [Google Scholar] [Publisher Link]

[90] Hamid Reza Baghaee et al., "Unbalanced Harmonic Power Sharing and Voltage Compensation of Microgrids Using Radial Basis Function Neural Network-Based Harmonic Power-Flow Calculations for Distributed and Decentralised Control Structures," *IET Generation, Transmission and Distribution*, vol. 12, no. 7, pp. 1518-1530, 2018. [CrossRef] [Google Scholar] [Publisher Link]

[91] Hamid Reza Baghae et al., "Nonlinear Load Sharing and Voltage Compensation of Microgrids Based on Harmonic Power-Flow Calculations Using Radial Basis Function Neural Networks," *IEEE Systems Journal*, vol. 12, no. 3, pp. 2749-2759, 2018. [CrossRef] [Google Scholar] [Publisher Link]

[92] David J. Perreault, R.L. Selders, and John G. Kassakian, "Frequency-Based Current-Sharing Techniques For Paralleled Power Converters," *IEEE Transactions on Power Electronics*, vol. 13, no. 4, pp. 626-634, 1998. [CrossRef] [Google Scholar] [Publisher Link]

[93] M. Hamzeh, H. Mokhtari, and H. Karimi, "A Decentralized Self-Adjusting Control Strategy for Reactive Power Management in an Islanded Multi-Bus MV Microgrid," *Canadian Journal of Electrical and Computer Engineering*, vol. 36, no. 1, pp. 18-25, 2013. [CrossRef] [Google Scholar] [Publisher Link]

[94] M.A. Parvez Mahmud et al., "Robust Nonlinear Distributed Controller Design for Active and Reactive Power Sharing in Islanded Microgrids," *IEEE Transactions on Energy Conversion*, vol. 29, no. 4, pp. 893-903, 2014. [CrossRef] [Google Scholar] [Publisher Link]

[95] Alfred Engler, "Applicability of Droops in Low Voltage Grids," *International Journal of Distributed Energy Resources*, vol. 1, no. 1, pp. 1-6, 2005. [Google Scholar]